




Review

Photocatalytic Membranes in Photocatalytic Membrane Reactors

Pietro Argurio ^{1,*} , Enrica Fontananova ^{2,*}, Raffaele Molinari ¹  and Enrico Drioli ^{2,3} 

¹ Department of Environmental and Chemical Engineering, University of Calabria, Via P. Bucci, 44/A, I-87036 Rende (CS), Italy; raffaele.molinari@unical.it

² Institute on Membrane Technology (ITM), National Research Council of Italy (CNR), Via P. Bucci Cubo 17C, I-87036 Rende (CS), Italy; e.drioli@itm.cnr.it

³ Center of Excellence in Desalination Technology, King Abdulaziz University, P.O. Box 80200, Jeddah 21589, Saudi Arabia

* Correspondence: pietro.argurio@unical.it (P.A.); e.fontananova@itm.cnr.it (E.F.)

Received: 2 August 2018; Accepted: 5 September 2018; Published: 7 September 2018



Abstract: The present work gives a critical overview of the recent progresses and new perspectives in the field of photocatalytic membranes (PMs) in photocatalytic membrane reactors (PMRs), thus highlighting the main advantages and the still existing limitations for large scale applications in the perspective of a sustainable growth. The classification of the PMRs is mainly based on the location of the photocatalyst with respect to the membranes and distinguished in: (i) PMRs with photocatalyst solubilized or suspended in solution and (ii) PMRs with photocatalyst immobilized in/on a membrane (i.e., a PM). The main factors affecting the two types of PMRs are deeply discussed. A multidisciplinary approach for the progress of research in PMs and PMRs is presented starting from selected case studies. A special attention is dedicated to PMRs employing dispersed TiO₂ confined in the reactor by a membrane for wastewater treatment. Moreover, the design and development of efficient photocatalytic membranes by the heterogenization of polyoxometalates in/on polymeric membranes is discussed for applications in environmental friendly advanced oxidation processes and fine chemical synthesis.

Keywords: photocatalytic membrane reactors; photocatalytic membrane; fine chemistry; wastewater treatment

1. Introduction

Membrane reactors (MRs) are multifunctional reactors that are characterized by the combination of a (catalytic) reaction with a membrane separation processes. The early examples of MRs date back to the 1970s with the use of polymeric membranes in enzymatic reactions and metal membranes for high temperature reactions [1]. Currently, MRs have relevant industrial applications in biotechnological field but also in the environment areas, such as wastewater treatment and gas emissions purification [2,3]. An interesting case is the membrane bioreactors (MBRs) technology recognized as a best available technology (BAT) for wastewater treatments [4]. However, in the last decades, a growing interest towards MRs technology is evident in a wide range of applications, including, not only biotechnological, but also petrochemical, chemical production, environmental remediation, and energy sector. Regarding the environment protection, MRs have been applied in different areas such as wastewater treatment by advanced oxidation processes (AOPs) for organic pollutants degradation and gas emissions purification for CO₂ capture [3]. The main driving force of these academic and industrial research efforts is the necessity to innovate the current resource within an intensive industrial system in the perspective of the sustainable growth.

The Process Intensification (PI) strategy [5,6] is recognized as an efficient tool for the realization of this sustainable growth. The PI strategy comprises an innovative equipment design and process development methods, being able to improve manufacturing and processing, by decreasing production costs, equipment size, energy consumption, waste generation, while improving process efficiency, remote control, information fluxes, and process flexibility [7]. MRs are specific example of reactive separations well responding to the requests of the PI strategy, coupling a reaction with a membrane separation process, not only at equipment level, but by realizing functional synergies between the operations involved [6]. This synergic combination can have several advantages in comparison with traditional reactors depending on the specific functions performed by the membrane [8]. With respect to traditional reactive separations (e.g., reactive distillation, reactive adsorption, reactive crystallization/precipitation), MRs have the advantage to use intrinsically more clean and energy-efficient separation routes [6]. Membrane separations are in fact typically characterized by lower operating temperature, in comparison with thermal separation processes, such as distillation, and they might offer a solution in the case of catalysts or products with a limited thermal stability. Additionally, membrane separation processes are able to separate nonvolatile components by a difference in dimensions, charge, or volatility.

The selective transport of the products and/or the reagents through the membrane can increase the yield and/or the selectivity of some processes. Typical examples are esterification and de-hydrogenation reactions (thermodynamically controlled reactions), in which the removal of water or hydrogen, respectively, increases the reaction yield. The extraction of an instable intermediate through the membrane in a MR might give an improvement of the reaction selectivity; this is the case of partial oxidation reactions and hydrogenation reactions carried out in MRs; also, the selective removal of the reaction products might also improve the downstream processing.

In the case of homogenous catalysts, their immobilization in or on a membrane represents an efficient way to achieve the catalyst recovery, regeneration, and reuse in successive catalytic runs [9].

The membrane can also define the reaction volume providing a contacting zone for two immiscible phases (e.g., in phase transfer catalysis) [10] avoiding the use of polluting auxiliaries, like solvents, in agreement with the green chemistry principles.

The design of the membrane reactor requires a multidisciplinary approach in which different disciplines, like: chemistry, chemical engineering, membrane engineering, and process engineering, give their contribution in order to achieve a synergic combination of the separation and reaction processes that allows optimal performances in terms of productivity and sustainability.

When a membrane is combined with a photocatalytic process the MR is indicated as photocatalytic membrane reactor (PMR) [11] and it can be designed in two main configurations, depending from the catalyst confinement [12–14]: (i) PMRs with solubilized or suspended photocatalyst; and, (ii) PMRs with photocatalyst immobilized in/on a membrane.

Both configurations present specific advantages and limitations depending from the specific application. In a PMR with a solubilized or suspended photocatalyst, a membrane with appropriate molecular weight cut off (MWCO) can be used for the retention of the catalyst in the reactor. Usually globular proteins in aqueous solution are used for MWCO measurements, however in the membrane selection it is necessary to consider that the MWCO depends on the solvent and the solution composition and polarity might change in relevant way during the reaction [10]. The catalyst retention can be optimized by enlargement of the catalyst as: dendrimers, hyperbranched polymers or catalyst bound to a soluble polymer [15]. Moreover, the membrane can have the multiple role of confining, the catalyst, the pollutants, and the degradation intermediates into the reaction environment. In a traditional photoreactor, the degradation intermediates remain in the treated effluent resulting often in a not sufficiently efficient process because these intermediates are frequently more hazardous than the original pollutants. The coupling of photocatalysis and membrane separation can permit to obtain, by using a membrane with an appropriate selectivity, a permeate free of both pollutants and degradation intermediates.

PMRs with solubilized/suspended photocatalyst can be further classified in: (i) integrative-type PMRs and (ii) split type PMRs. In the first one, the photocatalytic reaction and membrane separation processes take place in one apparatus, i.e., an inorganic or polymeric membrane is submerged in the slurry photocatalytic reactor. In split-type PMRs the photocatalytic reaction and membrane separation take place into two separate apparatuses, i.e., the photocatalysis module and the membrane module, which are appropriately coupled [12,16]. Besides, on the basis of a different approach, this kind of PMRs can be also classified while considering the position of the light source, which can be: (i) above/inside the feed tank; (ii) above/inside the membrane unit; and, (iii) above/inside to an additional vessel placed between the feed tank and the membrane unit [13].

In PMRs with immobilized photocatalyst, the photocatalyst is not solubilized/suspended into the reacting environment, but it is immobilized in/on the membrane, giving a photocatalytic membrane (PM). In such a system, the membrane acts both as a selective barrier for the contaminants to be degraded, thus maintaining them into the reaction environment, and as the support for the photocatalyst. PMRs with immobilized photocatalyst are intrinsically integrative-type PMRs, i.e., the photocatalytic and the membrane separation processes take place in the same unit.

In general, in the state of the art literature it has been reported that the PMRs with solubilized/suspended photocatalyst permit to achieve higher efficiency when compared to that of the immobilized system, due to the larger active surface area, which guarantees a good contact between the photocatalyst and the pollutants [12,14]. As a consequence, more numerous are the studies of PMRs with solubilized/suspended photocatalyst, in view of large scale applications [17–20]. However, fouling, which is caused by deposition of the photocatalyst nanoparticles (NPs) on the membrane surface with a consequent flux decline, and light scattering, still limits the performance of this type of membrane photoreactor configuration.

In the immobilized PMRs, the photocatalyst/reagents contact is hindered by the mass transfer limitation over the immobilized photocatalyst. However, in this configuration, it is possible to obtain in general a more easy catalyst recovery, reuse and regeneration in successive catalytic runs than in the previous one.

Besides, PMs generally show better performance with respect to conventional membranes in terms of reduced membrane fouling and improved permeate quality. PMs could degrade the organic pollutants contained into the feed solutions by generating the oxygen-reactive radicals under light irradiation, thereby preventing the formation of a cake layer on the membrane surface, reducing the pollutant concentration in the retentate as well as improving the permeate quality. Moreover, the problem of light scattering by photocatalyst particles, which negatively influence the performance of PMRs with suspended photocatalyst, is avoided by using PMs. So, it can be affirmed that the use of PMs might improve the performance of wastewater treatment by PMRs.

Significant progresses have been also reached in the modelling and simulation of membrane reactors with the aim to improve their performances by the optimization of the reactor design and the operative conditions, as well as, by the understanding and optimization of structural/functional relationships at a molecular level in the systems investigated. New metrics, like the volume index and conversion index, have also been proposed as a simple way to evaluate the efficiency of a membrane reactor in the logic of the process intensification strategy [21].

The present work gives a critical overview of the recent progresses and new perspectives in photocatalytic membranes and photocatalytic membrane reactors. The most important operating parameters affecting the performance of the PMRs are deeply discussed. Then, based on some selected case studies, the criteria for designing and developing a PM are reported. Finally, recent achievements in the use of visible light and in the overcoming of some intrinsic limitations of PMs, like moderate loss of photoactivity and restricted processing capacities, owing to mass transfer limitations and unsatisfactory system lifetime, due to photocatalyst leaching, are overviewed.

2. Operating Parameters and Limits of Photocatalytic Membranes (PMs)

Working under proper operating conditions is important to obtain good PMR performance with both solubilized/suspended and immobilized photocatalyst. The most important factors affecting the PMR performance, influencing the photocatalytic process and/or the membrane process, were reviewed by various authors [12–14]. These factors can be summarized, as follows.

2.1. Operating Mode

PMRs with immobilized photocatalyst can be operated in both dead-end and cross flow modes [22,23]. When the PMR is operated in dead-end mode, the substrates are retained by the membrane and accumulate on its surface thus forming a cake layer. As a result, the membrane permeability and the photocatalytic performance are reduced. Relatively low photocatalytic efficiency is usually observed by operating under dead end mode. This drawback can be explained, as follows: since the feed polluted water was kept into the reactor (no recirculation), a not adequate contact between the pollutants to be degraded, the photocatalyst and the light source was achieved.

On the basis of this, it can be affirmed that the cross flow mode should be the better option in view of industrial applications. By operating in this way, the feed phase flows tangentially to the membrane. This tangential flow tends to remove the deposited particles on the membrane surface, thus resulting in a reduced membrane fouling. The permeate flows perpendicularly across the membrane, while the retentate is usually recirculated in the feed tank.

2.2. Typology of Photocatalyst Immobilization

On the basis of the different procedure of photocatalyst immobilization, PMRs with immobilized photocatalyst can be further classified in three sub-categories.

The first sub-category comprises the PMRs in which the photocatalyst is coated on the PM. The procedure of coating can be performed by using different methods [24] such as dip-coating, electro-spraying of photocatalyst particles, magnetron sputtering of the photocatalyst, and deposition of gas phase photocatalyst NPs. The main drawbacks of using this approach are associated to the diminution of membrane permeability after the coating procedures and to photocatalyst leaching during the photocatalytic runs [25].

The second sub-category includes the PMRs in which the photocatalyst is blended into the membrane matrix. Practically in this kind of PMR, during the membrane preparation the photocatalyst is entrapped in the polymeric matrix. By operating with this type of PMRs, the possibility of photocatalyst leaching was reduced with respect to the PM that was prepared by photocatalyst coating.

The third sub-category of PMRs with immobilized photocatalyst is based on the use of free standing PM. In this case, the PM is manufactured with a pure photocatalyst, so that the immobilization of the photocatalyst in/on the membrane support is unnecessary. Thus, a further reduction of the possibility of photocatalyst leaching was obtained.

2.3. Photocatalyst Type and Its Characteristics

Photocatalyst is the key component of a photocatalytic process. The properties of photocatalyst and its concentration in the reacting environment represent key parameters, playing an important role on photocatalytic performance.

Key properties of photocatalyst, having significant effects on photocatalytic efficiency, are the band gap energy, the specific surface area and particle size distribution, the crystallographic structure and composition, etc.

A photocatalyst is a semiconductor material able to convert the energy of irradiated photons in the chemical necessary to excite electrons from its valence band (VB) to its conduction band (CB). Then, it is clear that band gap energy plays the most important role in its selection. A photocatalyst characterized by lower band gap requires less photon energy. In particular, a photocatalyst can achieve

a satisfactory visible light response when its band gap is sufficiently low, which is an important characteristic in view of large scale applications. Other important characteristics to be considered to choose a photocatalyst are good chemical and physical stability, non-toxic nature, availability, and low cost.

TiO₂-based photocatalyst is the most utilized photocatalyst in PMR (used in suspended form) because it is characterized by strong catalytic activity, relatively long lifetime of electron-hole pairs, high (photo)chemical stability in aqueous media and in a wide range of pH (0–14), limited cost, and low toxicity. So, it can be affirmed that TiO₂ is the archetypical photocatalyst, virtual synonym for photocatalysis. However, this material is not active under visible light irradiation, because of its wide band gap. Thus, TiO₂ is capable to use only less than about 5% of the solar energy, which is in the UV range. On these bases, the development of photocatalysts that are able to utilize visible light represents a challenge in view of large-scale application of PMR systems, permitting the use of a greener light source (the sun) [26,27]. When considering that the quantum efficiency of the photocatalytic processes usually decreases by increasing the intensity of the radiation, the preparation of photocatalysts active under visible light is convenient only when the quantum efficiency remains relatively high, resulting in a wide use of photons from visible light.

Other metal oxide semiconductors that are used in PMRs are ZnO [28,29], WO₃ [30], and CuO/ZnO [31]. These photocatalysts are characterized by a different band gap in comparison with TiO₂ [14].

Polyoxometalates (POMs) are instead soluble metal oxide analogs with tunable solubility depending from the counterion used [32]. The heterogenization of POMs in/on polymeric membranes for PMRs application is reviewed in Section 4.2.

2.4. Light Source

The starting step in a photocatalytic process is the irradiation of the photocatalyst surface with photons having energy ($h\nu$) equal to or higher than the band gap, so that the electrons are promoted from VB to CB. Several authors studied the influence of wavelength and intensity of the light source on the rate of the photocatalytic reaction [33–35].

The photocatalytic performance depends strongly on the value of the light intensity [36]. In general, it can be observed that the reaction rate increases by increasing the light intensity till to the mass transfer limit is achieved. In general, the reaction rate increases with the light intensity when the photocatalytic process is operated at low light intensity, which means a light intensity in the range 0–20 mW·cm⁻². This trend can be explained when considering that, by operating with this light intensity, the reaction giving the formation of electron-hole couples is predominant with respect to the electron-hole recombination. By operating with a light source emitting at medium light intensity (approximately 25 mW·cm⁻²), the reaction rate is function of the square root of light intensity. This trend can be ascribed to the competition effect between the electron-hole formation and recombination reactions. The reaction rate is not influenced by this parameter when the photocatalytic process is performed with a high light intensity (>25 mW·cm⁻²) [12,13].

The UV spectrum is usually divided into UV-A (315–400 nm), UV-B (280–315 nm), and UV-C (100–280 nm), depending on the emitting wavelength. Artificial UV lamps are the most commonly used light sources, because of their higher photon flux with respect to solar irradiation. These lamps can be used in immersed or external configuration, and emit light in the UV-A range (max intensity in the range 355–365 nm) or in the UV-C range (germicidal lamps, max intensity at 254 nm).

Depending on the emission range of interest, different typologies of light sources are available, like xenon, mercury, and deuterium lamps [37]. Besides, regarding the different radiation sources, it can be distinguished between pulsed and continuous light sources [38], which can affect the photocatalytic performance.

Several works on laser induced photocatalysis have been also recently carried out [38–40]. Yamani [38], compared the photocatalytic performance of 355 nm pulsed laser and continuous Hg

arc lamp equipped with visible light band pass filter. The results evidenced that the photocatalytic degradation efficiencies that were obtained with the different radiation sources were comparable and the pulse energy has an important influence on the photocatalytic performances.

Among the various types of lamps, the led ones, emitting in the UV or UV-vis range, are gaining interest for their efficiency and they can be also powered by photovoltaic panels [41].

2.5. Feed Characteristics

The properties of feed that influence the performance of a PMR with entrapped photocatalyst comprise the initial concentration of the pollutants to be degraded, the pH of the feed, the temperature, and the presence and concentration of inorganic ions.

It is generally accepted that the reaction rate increases with substrate concentration till to a certain level, over which the rate starts to decrease. This trend can be explained considering that a further increase of substrate concentration results in a reduction of the generation rate of $\bullet\text{OH}$ radicals due to light scattering by the dissolved substrate and to the decrease of the active sites available for $\bullet\text{OH}$ radicals generation (photocatalyst saturation).

In their study on photocatalytic degradation of the dye tartrazine, Aoudjit et al. [42] evidenced that the dye concentration in the feed phase to the PMR system strongly affects system performance. Indeed, the photodegradation percentage decreased from ca. 78 to 46% by increasing the initial concentration of the dye from 10 to 30 $\text{mg}\cdot\text{L}^{-1}$. This trend was explained by considering that, maintaining the amount of the photocatalyst constant, the ratio hydroxyl radical/tartrazine molecules decreases by increasing dye concentration, resulting in the lower photodegradation efficiency observed. Moreover, the higher tartrazine concentrations also increase the light scattering, thus affecting the UV light absorbance by TiO_2 nanoparticles surface and decreasing the amount of hydroxyl radicals formed.

The increase of the initial substrate concentration influences not only the photocatalytic performance of the system, but also the fouling of the membrane, and thus the permeate flux. So, also when the increase of pollutants concentration has a positive effect on the photodegradation rate, it has to be taken into account that the mass transfer resistance of the membrane also increases, resulting in the deterioration of membrane performance [43].

The operating pH strongly influences the performance of a PM. First of all, the adsorption of the substrate on the active sites of the photocatalyst and desorption of the products are two pH-influenced processes. In the case of the TiO_2 -Degussa photocatalyst, considering that its isoelectric point is 6.8, it can be affirmed that a TiO_2 based PM is negatively charged when the pH of the feed solution is higher than 6.8. In this condition, the adsorption of positively charged molecules is favored. On the contrary, the TiO_2 based PM is positively charged when the pH of the feed phase is lower than 6.8, and the adsorption of negatively charged substrates is favored. The operating pH also influences the permeation of the different solutes contained into the feed solution across the membrane. Indeed, the molecules dissolved in the reacting environment could change their state from positively charged to neutral, and then from neutral to negatively charged by changing the pH, having an important effect on their permeation across the membrane.

It is accepted that a temperature in the range 20–80 °C is optimal for conducting photocatalytic processes [33]. By operating at temperature lower than 0 °C, the desorption of the photodegradation products from the surface of the photocatalyst becomes the limiting step, and the photocatalytic activity decreases. On the other hand, at a temperature higher than 80 °C, the electron-hole recombination on the photocatalyst is favored, which has a negative effect on photocatalytic efficiency. Besides, at those higher temperatures the adsorption of the substrate (exothermic process) is inhibited.

The presence of inorganic ions in the feed solution can give positive or negative effects on the rate of the photocatalytic process depending on the reaction mechanism and its nature. In particular, the presence of inorganic ions as Cl^- , NO_3^- , SO_4^{2-} , CO_3^{2-} and HCO_3^- , which usually exist in waters, decreases photocatalytic activity by scavenging holes (h_{CB}) and hydroxyl radical ($\bullet\text{OH}$) [44–46]. On the other hand, the addition of oxyanion oxidants, such as $\text{S}_2\text{O}_8^{2-}$, BrO_3^- , IO_4^- , ClO_2^- , and ClO_3^- ,

has a positive effect on the photoreactivity. Indeed, these ions could act as scavenger for the CB electrons and reduce the electron-hole recombination, as follows:



H_2O_2 is another oxidant species that increases the photoreactivity of the system, thanks to the formation of $\bullet\text{OH}$ radicals. Nevertheless, as reported by some authors [47] an excessive amount of hydrogen peroxide can have a negative effect on system reactivity. This behavior can be explained considering that H_2O_2 acts as scavenger of VB holes and $\bullet\text{OH}$, producing hydroperoxyl radicals ($\text{HO}_2\bullet$) as follows:



The $\text{HO}_2\bullet$ radical has a less oxidizing power than $\bullet\text{OH}$.

The presence of inorganic ions into the feed solution, affecting the photocatalytic performance as described, can also influence the performance of the membrane separation process. The influence of inorganic salts and humic acids on fouling and stability of a polyethersulfone ultrafiltration (UF) membrane operated in a PMR was studied by Dorowna et al. [48]. A more significant influence of inorganic ions on membrane performance was observed by increasing the concentration of the salts.

2.6. Flow Rate over and across the Membrane

In the case of PMRs that operated under cross-flow filtration mode, where the feed solution is continuously recirculated tangentially to the membrane, the recirculation flow rate is an important operating parameter affecting the photocatalytic performance of the system. Usually, the photocatalytic efficiency increases by increasing the recirculation flow rate. This trend can be explained by considering the larger turbulence in the solution, which promotes the mass transfer from the bulk of the feed solution to the surface of the PM, while reducing the membrane fouling.

Flow rate across the membrane depend on the applied driving force (e.g., transmembrane pressure in a pressure driven membrane separation), membrane structure, and composition. It is a key parameter for the PMR because it determines the contact times between the photocatalyst and the reagents/products. Mass transfer of the reagents to the catalytic sites, and of the product away from them, should be fast enough in order to avoid reaction limitation meanwhile the contact time catalyst/reagent should be also appropriate to control reaction selectivity.

3. Preparation and Choice of Materials to Manufacture PMs

An “ideal” (photo)catalyst should conjugate the following properties: low costs, high selectivity, elevated stability under reaction conditions, non-toxicity and “green properties”, like “recoverability”, i.e., the possibility to recover and reuse the catalyst [49,50]. In this perspective, the heterogenization of homogeneous catalysts in/on a support has interesting implications because it permits to recover and reuse the same catalytic system several times. Among the different heterogenization techniques, the entrapping of a catalyst in or on a membrane offers new possibility for the design of new efficient catalytic processes.

In the design of a catalytic membrane major issues in the membrane material selection are the mechanical, thermal and chemical stability under reaction conditions. In the case of photocatalytic membranes also the photostability and transparency of the membrane are critical concerns. Moreover, the membrane transport properties, like permeability and selectivity, need to be considered and can be tailored by an appropriate selection of the membrane structure and composition. In the case of a (photo)catalytic membrane, the incorporation of the (photo)catalyst introduces additional complexity to the fabrication process, because the catalyst should be firmly entrapped in the membrane and

the catalyst structure and activity has to be preserved during the membrane preparation procedure. Moreover, the properties (including transport properties) of a catalytic membrane are usually different from those of a pristine polymeric membrane that is prepared in the same experimental conditions.

A variety of materials have been used for the preparation of PMs: organic, inorganic, and metallic. In particular, polymeric membranes represent the most popular organic materials used to prepare PMs. Typical polymers that have been considered as membrane material include polyamide [51], polyvinylidene fluoride (PVDF) [52], polyethersulfone (PES) [53], polyurethane (PU) [54], polyethylene terephthalate (PET) [55], polyacrylonitrile (PAN) [56], and polytetrafluoroethylene (PTFE) [57].

Since the PM is in direct contact with the reacting environment, the possibility of its damage by the irradiation and oxidizing species (e.g., $\bullet\text{OH}$ radical) has to be taken into account. More often, the abrasion of membrane surface because of the mechanical action of the particles suspended in the reacting environments causes more damage to the membrane than the action of the oxidant environment [58]. On the basis of this, inorganic ceramic membranes, thanks to their excellent thermal, chemical, and mechanical stability, may represent a good option to polymeric membranes in PM preparation. Actually, the main limitation to ceramic membrane utilization is represented by the higher manufacturing cost when compared to polymeric membrane.

It is important to realize a stable catalyst immobilization in order to avoid catalyst leaching out from the membrane and to have a good adhesion between the membrane material and the catalyst, with an optimal dispersion of the second one. Different immobilization strategies can be used in order to achieve these goals. Covalent bindings in general guarantee a stable immobilization. However, also electrostatic interactions, weak interactions (Van der Waals or hydrogen bonds), or catalyst encapsulation are exploited for an efficient catalyst immobilization [59].

In several cases, the catalyst is immobilized during membrane formation processes by dispersing the catalyst in the polymer dope solution. The polymer/catalyst affinity can be tailored by an appropriate chemical functionalization of one or both components. Ideally, the solvent used for the reaction needs to be a non-solvent for the catalyst, and it is necessary that the membrane does not swell excessively.

For a porous membrane, the choice of the membrane material is of less importance for transport properties in comparison with a dense membrane, because permeation occurs through the membrane pores [10]. However, the membrane material is relevant for the membrane stability, as well as for wettability and fouling tendency.

The membrane preparation technique and conditions depend from the membrane material and the desired structure and morphology. Different techniques for membrane preparation can be opportunely employed to prepare catalytic membranes: phase separation, coating, interfacial polymerization, sintering, stretching, and track-etching, are some examples [60]. The most used and versatile for polymeric membranes is the phase separation technique.

3.1. Dip Coating with Photocatalyst Particles

A widely employed surface immobilization technique consists in dip coating. Wang et al. [61] studied the synthesis of high quality TiO_2 membranes on alumina supports and tested the so prepared PMs in the degradation of the dye Methyl Orange (MO). In particular, the PMs were synthesized by the spin-coating technique using the sol-gel method with water-soluble chitosan (WSC) as an additive. Obtained results evidenced that the proposed method of preparation permitted obtaining TiO_2 membranes on alumina supports that were characterized by enhanced structural and catalytic properties. High surface area ($116\text{--}164\text{ m}^2\cdot\text{g}^{-1}$) and porosity ($47.3\%\text{--}52.2\%$) were obtained, as well as homogeneity without cracks and high degradation of MO ($61.2\%\text{--}49.2\%$).

Chakraborty et al. [62] immobilized TiO_2 NPs on polymeric hollow fibers (HFs) UF membranes while using three immobilization methods: (i) spray coating, (ii) vacuum coating, and (iii) sol-gel dip coating. PES and polyvinylchloride (PVC)-PAN HF membranes were used as catalyst support.

In the case of spray and vacuum coating, a significant leaching/detachment of NPs has been observed. This result was explained by the authors while considering that the NPs were immobilized physically and not chemically. Thus, a not stable coating on the membrane surface was obtained. Besides, spray coated and vacuum coated PMs showed negligible permeability due to the clustering of TiO₂ adding extra resistance layers to water permeation across the membrane and to the blocking of the membrane pores by TiO₂ agglomerates, respectively. This was also confirmed by Scanning Electron Microscopy (SEM) images.

The sol-gel coating was tested as the third method of photocatalyst immobilization on the membrane surface. In this case the coating solution was a diluted sol, coated on the membrane by using a simple lab-scale dip coater. The coating method was optimized in order to obtain a better immobilization of TiO₂ NPs on the membrane while limiting the permeability loss in the coated membrane. SEM images and Raman spectra confirmed TiO₂ immobilization on the polymeric support and evidenced that sol-gel coating permitted obtaining a stable TiO₂ layer. The pure water permeability of the coated membranes was about 65–80% below those of uncoated membranes for both PES and PVC-PAN.

3.2. Electrospraying of Photocatalyst Particles

Daels et al. [51] prepared polyamide nanofiber membranes containing TiO₂ NPs by electrospinning. The photocatalytic activity of the prepared PMs was demonstrated by considering the photodegradation of the dye MB. The results of photodegradation (up to 84% after 2 h of UV irradiation) evidenced the excellent photocatalytic activity of TiO₂ NPs immobilized on the nanofibrous structure. After 6 h of UV irradiation the photocatalytic degradation increased up to 99%, thus obtaining a quantitative removal of MB. The stability of the PMs was confirmed, demonstrating that the NPs of the photocatalyst were successfully incorporated onto the electrospun fibers.

By using a similar approach, Nor et al. [63] prepared electrospun PVDF/titanium dioxide nanofibers (PVDF/TNF) by hot pressing TNF onto PVDF flat sheet membrane. The membranes were prepared by three consecutive steps. First of all, the polymeric support, i.e., the flat sheet PVDF membrane was prepared by a slight modified diffusion phase inversion technique. Then, the TiO₂-NFs were synthesized by the electrospinning technique at room temperature. The spun TiO₂-NFs were collected on an aluminum foil. Finally, the TiO₂-NFs were placed and hot pressed for 30 min onto the PVDF membrane. The hot press technique was carried out at constant pressure (80 bar) by varying the operating temperatures (60 °C, 100 °C, 160 °C, and 180 °C). The membranes that were hot pressed at 60 °C exhibited unfavorable structure, since the TiO₂-NFs were not adhered completely.

3.3. Sputtering of Photocatalyst Particles

Another possible technique for manufacturing PMs with the photocatalyst coated on the solid support is represented by sputtering a titanium film on top of the membrane [64]. By using this approach, Fischer et al. [65] easily synthesized TiO₂ nanotubes by sputtering a titanium film on top of a porous polymer material, namely a PES membrane. The sputtering step was followed by the anodization of titanium to TiO₂ nanotubes and the subsequent crystallization to photocatalytically active anatase under mild conditions (temperatures below 120 °C). The so-prepared PMs were characterized by a photocatalytic activity increased up to six times when compared to a TiO₂ film on the membrane. This result was ascribed to the enhanced surface area and light-harvesting capability of the anatase nanotubular structures on the membrane.

3.4. Deposition of Gas Phase Photocatalyst Nanoparticles

PMs coated with nanostructured thin films of TiO₂ and Pt/TiO₂ have been also produced by one-step deposition of gas phase NPs on glass fiber filters [66]. The obtained PMs, coated with Pt/TiO₂ nanostructured films, were tested in the photocatalytic hydrogen production by ethanol photo-steam reforming. An increased reaction rate with respect to that obtained with the same

photoactive Pt/TiO₂ films deposited by using more conventional methods on a quartz substrate was observed. This enhanced H₂ production rate was ascribed to the increased contact time of the reactant mixture with the photoactive films, thanks to the diffusion through the coated glass fiber filters.

The described methods permit obtaining coated PMs, where the photocatalyst is coated tightly on the surface of the support membrane. The main limitations of these photocatalytic systems consist in photocatalyst leaching and in the diminution of membrane permeability because of the increased membrane resistance.

3.5. Blended and Free-Standing PMs

In the case of blended PMs, the photocatalyst is blended into the membrane matrix. By operating in this way, the possibility of photocatalyst leaching is reduced when compared to coated PMs. The most used membranes for the photocatalyst entrapment were PVDF polymeric membranes [67,68]. Other polymeric membranes were also used [69–71]. Aoudjit et al. [42] prepared poly(vinylidene fluoride–trifluoroethylene) (P(VDF–TrFE)) PMs containing titanium dioxide P25 by solvent evaporation (see Figure 1). The analysis of the PM morphological properties evidenced an interconnected porous microstructure and the homogeneous distribution of the TiO₂ NPs within the membrane pores.

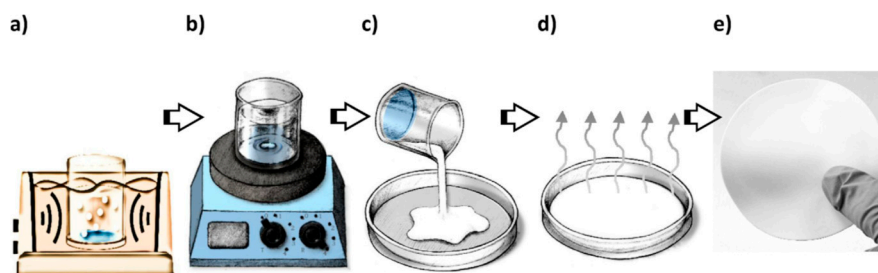


Figure 1. Schematic representation of the preparation of TiO₂/poly(vinylidene fluoride–trifluoroethylene) (TiO₂/PVDF-TrFE) nanocomposite photocatalytic membranes (PMs) by solvent casting; (a) ultrasonic bath of *N,N*-dimethylformamide (DMF) and TiO₂ nanoparticles (NPs); (b) magnetic stirring of DMF, TiO₂ NPs, and PVDF-TrFE; (c) pouring of the solution on a glass support; (d) solvent evaporation at room temperature; and, (e) membrane after complete evaporation of the solvent (Aoudjit et al. [42]).

The production of free-standing PMs, in which the PM is manufactured with a pure photocatalyst, is often performed via the electrochemical anodization of a metallic substrate of the photocatalyst, followed by the separation of the photocatalyst nanotube film and different annealing treatments. Compared to coated or blended PMs, in the case of free-standing PMs the immobilization step is unnecessary, thus further reducing the possibility of photocatalyst leaching. On this topic, Zhao et al. [72] designed and prepared crystallized doubly open-ended Ag/TiNT (NT: Nano Tube) array membranes. The PMs were prepared by a lift-off process. It was based on an anodization-annealing-anodization-etching sequence, followed by uniform Ag NPs decoration. The prepared PMs were tested in the photocatalytic degradation of gaseous *N,N*-dimethylformamide (DMF), which is a typical volatile organic compound contained in the gaseous effluents from manufacturing factories, obtaining very interesting results.

As reported, in view of efficient utilization of PMs, it is fundamental to prepare systems with appropriate stability, porosity, and durable immobilization of the catalyst particles. When considering these features, the implementation and use of fiber based membranes represent an interesting and promising approach in view of enhancing the photocatalytic activity of PMs [73].

4. Selected Case Studies

4.1. Ti- and Ag-Based Photocatalytic Membrane Reactors

The pioneering studies on the use of TiO₂-based membranes in photocatalytic membrane reactors were performed by Anderson and coworkers [74,75] about 30 years ago.

Molinari et al. [76] in 2002 entrapped TiO₂ photocatalyst in a polymeric membrane and compared the performance of the PM with that one obtained by using the same photocatalyst in suspension. The used light source was a medium pressure Hg lamp emitting in the range between 300 and 400 nm with a maximum emission peak of 366 nm. The photocatalytic efficiency of the entrapped catalyst was lower with respect to that of the suspended configuration. The presence of the polymeric chain around the particles of catalyst was the main cause of this trend, since it reduces the surface area of the photocatalyst that is available for light irradiation and substrate adsorption. The attack of •OH radicals to the PM represented another disadvantage of this system in which the photocatalyst was entrapped in polymeric membranes. The comparison of the results that were obtained by degrading different pollutants evidenced that the photodegradation rate was influenced by the presence of the reaction intermediate into the reacting environment. These molecules competed with the photocatalyst for light adsorption and with the substrate for catalyst adsorption.

Some important features of inorganic membranes are their higher chemical, thermal, and mechanical stability, with respect to the polymeric materials. Starting from this consideration, Zhang et al. [77] prepared, by using the sol-gel technique, TiO₂/Al₂O₃ PMs and tested them in the degradation of the azo-dye Direct Black 168 (DB). A high-pressure mercury lamp, with a maximum emission at 365 nm, was used as radiation source. The photolytic degradation of the dye achieved 70% and dye retention of the membrane was 65%, after 300 min by operating in continuous. The removal efficiency of the dye was improved markedly by coupling the UV irradiation with membrane filtration, and reached 82% after 300 min of UV irradiation, evidencing a synergistic effect. As emphasized by the authors, these TiO₂/Al₂O₃ composite PMs permitted to perform at the same time the photocatalytic degradation and the separation, obtaining a high permeate flux (82 L · m⁻² · h⁻¹) under low pressure (0.5 bar), while preventing membrane fouling, thanks to the high porosity and pore size of the PM. Despite these important achievements, the permeate quality was not excellent, evidencing that the membrane possessed an inadequate rejection to the pollutant.

The possibility to use a green light source, like the sun, to activate the photocatalyst represents a fundamental step in view of applying PMR systems at large scale. Thus, it is of great importance to develop immobilized photocatalytic systems with high quantum efficiency under visible light. In this direction it has to be taken into consideration that the increase of the radiation intensity usually causes a decrease of the quantum efficiency of the photocatalytic processes, which means a narrow use of photon from visible light.

On this topic, Athanasekou et al. [26] prepared and tested three kinds of active photocatalytic ceramic UF membranes. These PMs were prepared by dip-coating on the internal and external surface of UF mono-channel monoliths three different TiO₂ bases photocatalyst: nitrogen doped TiO₂ (N-TiO₂), graphene oxide doped TiO₂ (GO-TiO₂) and organic shell layered TiO₂. The photocatalytic activity of these PMs in the degradation of two azo dyes, MB and MO, was evaluated in a photocatalytic device operating in continuous dead-end conditions. Both the internal and the external side of the PMs were irradiated. The external side (shell) of the PMs was irradiated with two different radiation sources: (i) near-UV radiation in the range 315–380 nm, with a maximum emission at 365 nm; and, (ii) visible light. 10 UVA miniature LEDs emitting in the range 360–420 nm or six visible LEDs emitting at 460 nm were used to irradiate the internal side (lumen) of the PMs. The results evidenced that all the PMs were effective against common problems encountered in dye removal by conventional membrane filtration, like fouling tendency, increased energy consumption and the formation of retentate effluents containing the pollutant at high concentration. Best dye degradations (57% and 27% for MB and MO) were obtained by using the N-TiO₂ PM under UV irradiation. These unsatisfactory degradations

of the dyes gave evidence that the used PMs are not adequate for rejecting the dyes, despite the photocatalyst deposition. Lower dye degradations (29% and 15% for MB and MO, respectively) were obtained by using the same PM under visible light, despite the higher light irradiation density (7.2 vs. 2.1 $\text{mW}\cdot\text{cm}^{-2}$). This result evidenced that the N-TiO₂ PM did not achieve efficient quantum efficiency under visible light. By considering the cost of the process in terms of energetic consumption, the GO-TiO₂ membrane was the best one. Indeed, the energy consumption of GO-TiO₂ PM was only 28% when compared with that of consumed by the N-TiO₂ PM while providing 63% rejection of MB of N-TiO₂ PM. On this basis, it can be affirmed that the GO-TiO₂ PM can permit to achieve a higher dye rejection with a lower power energy consumption by recycling two or more times the permeate.

Considering the inadequateness in terms of pollutant rejection of the PMs prepared by Athanasekou, Wang et al. [78] prepared and tested in an experimental set-up operated under dead-end mode N-TiO₂ ceramic PMs characterized by higher photocatalytic efficiency. These PMs were synthesized by dip coating, similarly to Athanasekou et al., with a substantial difference: the dip-coating of the photocatalyst NPs on membrane support was repeated seven times. Thus, composite PMs characterized by an average pore size of ca. 2 nm, adequate for retaining the dye, were synthesized. SEM and X-Ray Diffraction (XRD) analyses evidenced that the doping of the TiO₂ photocatalyst with N permitted obtaining small nanocrystals with high surface and interfacial area. This feature, due to the inhibition of the growth of TiO₂ crystal grains by N doping, permitted obtaining improved photocatalytic performance. In particular, a permeation flux equal to ca. 96% of pure water flux, a close to 99% dye rejection and good membrane stability were obtained. Despite these interesting achievements, a rapid diminution of dye rejection, probably caused by the formation of cake layer and concentration polarization, was observed. This trend was ascribed to the used filtration mode. Besides, the N-TiO₂ PMs showed an unsatisfactory photoactivity under visible light.

On the same topic, Aoudjit et al. [42] prepared some PMs by immobilizing TiO₂-P25 NPs into a poly(vinylidene fluoride–trifluoroethylene) (P(VDF-TrFE)) membrane. The prepared NPs were tested in the photocatalytic degradation of tartrazine in the solar photoreactor schematized in Figure 2.

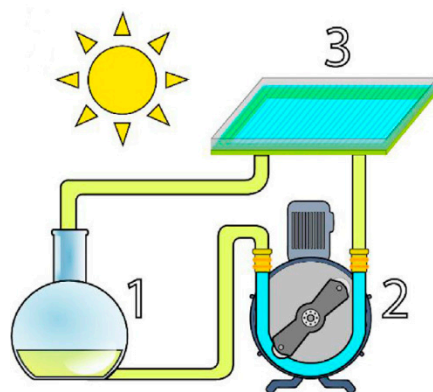


Figure 2. Schematization of the proposed solar photoreactor: 1—flask containing tartrazine solution; 2—peristaltic pump; and, 3—photoreactor containing the PM (Aoudjit et al. [42]).

The method used to prepare the P(VDF-TrFE) PMs was solvent evaporation, as described in Section 3. The photocatalytic degradation tests were performed in a solar photoreactor sited in northern Algeria, during August and September, under solar irradiation. The effective volume of the photoreactor was 1 L. The tartrazine solution was continuously recirculated at $28 \text{ mL}\cdot\text{s}^{-1}$ flow rate. Obtained results evidenced that the PM containing 8 wt.% TiO₂ was the best one, exhibiting a remarkable sunlight photocatalytic activity, with 78% of the pollutant degraded over five hours. As reported in Section 2.5, the initial dye concentration strongly affected system performance. In particular, the photodegradation efficiency decreased from 78 to 46% by increasing the initial dye concentration from 10 to 30 $\text{mg}\cdot\text{L}^{-1}$ because of: (i) the decreased ratio hydroxyl radical/tartrazine molecules; and, (ii) the higher light scattering, which affects the adsorption of UV light by the surface of

TiO₂ NPs, thus decreasing the amount of •OH formed. The degradation percentage of the considered dye after 5 h of irradiation was 37% and 77% for 9.78 and 28 mL·s⁻¹, respectively. This trend confirms what is reported in Section 2.6, i.e., the recirculation flow rate strongly influences the photocatalytic performance of the PM. This trend was due to the presence of more turbulence in the solution, which promoted the mass transfer from the feed solution to the surface of the PM. The reusability of the produced PM was also checked. Obtained results evidenced a 10% of efficiency loss by passing from the first use of the PM (ca. 78% of dye degradation) to the second use (ca. 67% of dye degradation). The observed efficiency loss was ascribed to photocatalyst leaching both during the photocatalytic tests and during the system cleaning with distilled water. However, no further reuses were possible because of the relevant leaching out of the NPs. The obtained dye degradations, unsatisfactory by an environmental point of view, were interesting by considering that they were obtained by using natural solar light.

Multi-walled carbon nanotubes (MWCNTs) are characterized by interesting properties, such as huge surface area, great electronic mobility, and stability. These characteristics make this material a good additive for preparing photocatalytic systems that are characterized by satisfactory photocatalytic activity and stability. On the basis of this and always with the aim of using solar radiation Wu et al. [79] prepared, by combining the electrospinning technique with an in situ reaction to obtain Ag₃PO₄, ternary composite fiber membranes (TCFMs), which possessed good photocatalytic performance. These TCFMs were composed by MWCNTs and Ag₃PO₄ supported on PAN. The results evidenced that the addition of MWCNTs into the Ag₃PO₄/PAN binary composite fiber membranes (BCFMs) is fundamental for obtaining a PM that is active under visible light. Indeed, the band gap of Ag₃PO₄/PAN BCFMs decreased by adding MWCNTs, making the ternary system able to use light characterized by higher wavelengths. The photocatalytic activity and stability of the prepared PMs were evaluated in a batch processing system by using a Xenon arc lamp. The emitted radiation was filtered with a 420-nm cut-off filter. Rhodamine B (RhB) was considered as model contaminant. By operating with the MWCNTs/Ag₃PO₄/PAN TCFMs, the RhB solution gradually discolored and the dye concentration drastically decreased and became practically zero after 80 min. When compared with the binary system, the ternary system was characterized by a higher and more stable photocatalytic activity for degrading RhB. In particular, the kinetic constant of dye degradation, calculated for the ternary system after observing that the degradation follows pseudo-first-order kinetics model, was 1.8-fold higher than that of the binary system. This result was ascribed to the fast electron transfer from Ag₃PO₄ to MWCNTs, resulting in a reduced electron-hole recombination and less photocorrosion of Ag₃PO₄.

Regarding system stability, the photocatalytic efficiency of TCFMs quantified in terms of dye removal after three recycles decreased by 20%, instead of the 45% decrease that was obtained without the MWCNTs. The slight decline of the activity was ascribed by the authors to the leaching of some Ag₃PO₄ NPs. When considering the photodegradation mechanism, it was observed that holes (h⁺) and superoxide radicals (•O₂⁻) played fundamental functions for degrading RhB.

The possibility of continuously degrading RhB by using flexible TCFMs under visible-light irradiation was checked in a PMR operated under dead end mode. On the basis of the results that are summarized in Table 1, it can be affirmed that the most important operating parameter affecting the removal rates was the initial RhB concentration. While considering the influence of initial RhB concentration in the feed solution on the removal percentage, it is confirmed that the reaction rate increases with substrate concentration till to a certain level, over which the rate starts to decrease. This trend, as reported in Section 2.4, can be ascribed to both diminution of •OH/pollutant molar ratio and light scattering, which reduced the production rate of •OH. The increase of the solution flow rate was also able to improve the removal percentage (Table 1).

Table 1. Influence of feed flow rate and initial RhB concentration on the photocatalytic degradation of RhB by using the MWCNTs-1%/Ag₃PO₄/PAN TCFMs (data from Wu et al. [79]).

Flow Rate (mL·min ⁻¹)	Feed RhB Concentration (mg·L ⁻¹)	Removal Percentage (%)
10	2	88.3
30	2	89.4
50	2	96.9
30	1	89.9
30	4	96.4
30	8	54.4

As emphasized by the authors, the overall results showed a high potentiality in continuous wastewater treatment when using a sustainable PMR. Modified methods to further improve the intensity of the interaction between Ag₃PO₄ NPs and fibers have to be employed for reducing leaching problems and increasing the stability of the photocatalytic performance.

The influence of salts and dissolved organic matter on the performance of PMs is another crucial point to be considered in the view of developing photocatalytic processes that are applicable at a large scale. Indeed, these substances, which are frequently present in real industrial effluents, can affect system performance by decreasing photocatalytic performance, due to scavenging effects, and/or by increasing membrane fouling.

On these aspects, Pastrana-Martínez et al. [27] determined the influence of dissolved NaCl on the performance of three PMs, indicated as M-P25, M-TiO₂, and M-GOT. These membranes were obtained by immobilizing on a plane cellulosic membrane TiO₂ P25, a lab-made TiO₂ and TiO₂ modified with graphene oxide (GO-TiO₂). These PMs were tested for photodegrading MO. A medium pressure mercury vapor lamp was used to operate under a near UV irradiation. A 430 nm cut-off filter was used for performing the experiments under visible light irradiations. The tests were performed in continuous under dead-end filtration. Three different aqueous matrices, distilled water (DW), simulated brackish water (SBW, 0.5 g·L⁻¹ NaCl), and seawater (35 g·L⁻¹ NaCl) were considered.

In Figure 3, the results that were obtained by using DW as aqueous matrix are summarized. The photocatalytic activity of M-GOT PM for MO abatement was higher than the other. This trend was also confirmed in terms of total organic carbon (TOC) removal. By using DW as aqueous matrix, MO abatement and permeate flux for two successive use were practically constants, regardless of the used PM. This result evidenced the maintaining of the photocatalytic activity of the tested PMs (membrane stability) without fouling problems. Practically, by using DW as the solvent, the photodegradation intermediates did not accumulate on the membrane surface. Thus, high permeate fluxes can be maintained by the PMs for long operation periods. The activity of M-P25 and M-TiO₂ membranes under visible light were negligible, while the M-GOT PM possessed a moderate visible light activity, due to the decrease of the band gap. The lower degradation that was obtained by operating under visible light was due to the lower light intensity entering into the photoreactor (2.8 vs. 33 mW·cm⁻²).

The presence of NaCl in SBW (0.5 g·L⁻¹) lead to a little decrease of photodegradation performance with respect to the use of DW, regardless of the PM employed. This trend was ascribed to Cl⁻ ion, having a scavenging effect on holes and hydroxyl radicals. This trend was also confirmed by TOC removal. However, the better performance (52% and 13% MO degradation for near UV-vis and visible light irradiation, respectively) was obtained by using the M-GOT PM. Moreover, the photocatalytic performance decreased from the first to the second use, confirming that chlorine anions act as scavengers of holes and hydroxyl radicals.

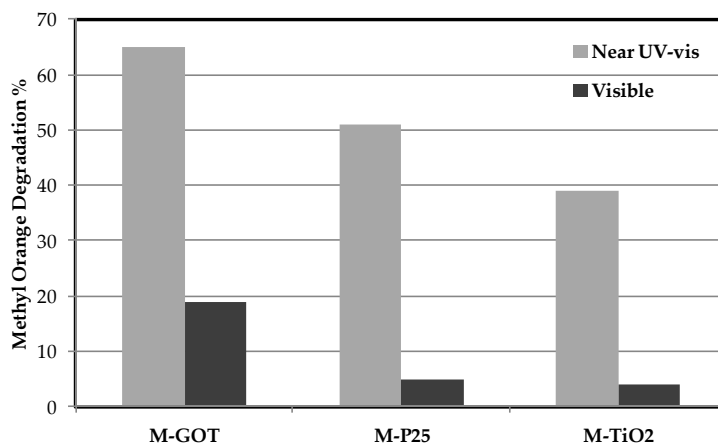


Figure 3. Photocatalytic degradation of Methyl Orange (MO) in distilled water (DW) in continuous mode under near UV-vis and visible light irradiation (data from Pastrana-Martínez et al. [27]).

The authors observed that, despite the encouraging results, these PMs showed lower photocatalytic efficiency with respect to PMRs with photocatalyst in suspension, as also evidenced in other works [80,81].

Fiber based membranes are characterized by good porosity and efficient dispersion and stabilization of catalyst NPs into the solid matrix. On the basis of this, Papageorgiou et al. [73] prepared and tested for MO degradation Ca alginate polymer fibers, which represent good candidates for photocatalytic applications thanks to some of their properties as the possibility to achieve good porosity together with the high transparency of their matrixes.

The results that were obtained during preliminary batch tests evidenced that Ca alginate/TiO₂ fibers possessed a photodegradation efficiency (measured in terms of MO degradation) higher than that of TiO₂ powder. This result was attributed to the good adsorption capacity and the high surface area of the fibers coupled with the excellent dispersion and stability of the TiO₂ NPs into the solid matrix. Despite these encouraging results, Ca alginate/TiO₂ polymer fibers gradually degraded, because of the •OH attack on the polymeric material, as previously observed by Molinari et al. [76].

Continuous flow experiments were performed in the hybrid photocatalytic/UF experimental set-up schematized in Figure 4, where a photocatalytic UF membrane (UF-PM) was coupled with the composite Ca alginate/TiO₂ porous fibers. The UF-PM was obtained by chemical vapor deposition of TiO₂ NPs on both the surfaces of a γ -alumina UF support. As evidenced in Figure 4, the permeate effluent, which represents the treated water, was collected inside the UF-PM, indicated as tubular membrane (Figure 4). 15 UVA LEDs emitting in the UV range 360–420 nm with a maximum emission peak at 383–392 nm irradiated the internal surface of this membrane. The polluted water has been fed in the lumen of Ca alginate/TiO₂ polymer fibers in a flow channel that is defined by the intermediate and the outer Plexiglas tubes (Figure 4). Four UV lamps emitting in the near-UV range 315–380 nm with a maximum emission peak at 365 nm, were used to irradiate the alginate fibers.

The TiO₂/Ca alginate fibers, working as pretreatment stage of the UF-PM, permitted to obtain an increase of the photocatalytic efficiency in comparison with the use of the UF-PM alone. Moreover, these photocatalytic active fibers in the process permitted obtaining an increased permeate flux across the UF-PM. The degraded Ca alginate/TiO₂ polymer fibers were retained by the UF-PM, thus preventing permeate quality deterioration. Despite these advantages that were achieved thanks to the use of these fibers as pretreatment stage, an unsatisfactory 40% dye removal was obtained.

Summarizing, it can be affirmed that particle agglomeration, which is an important drawback of TiO₂ promoted photocatalysis, can be limited/eliminated by developing TiO₂-nanofiber (TiO₂-NF). Despite this achievement some fundamental aspect have to be addressed in view of industrial application: (i) the degradation of the TiO₂/Ca alginate fibers, which affects both permeate quality and system lifetime, and (ii) the poor dye removal meaning unsatisfactory permeate quality.

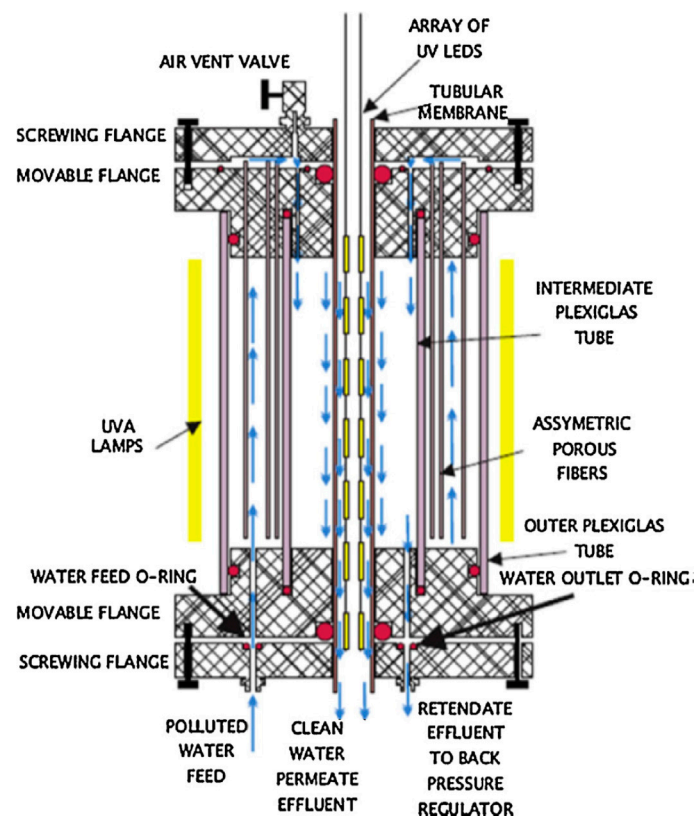


Figure 4. Schematization of the hybrid experimental set-up used by Papageorgiou et al. [73].

On the same topic, Nor et al. [63] prepared nanocomposite PMs consisting of TiO_2 nanofibers (TiO_2 -NFs) electrospun on PVDF supports. The photocatalytic efficiency of these PVDF/ TiO_2 PMs was evaluated in the photocatalytic degradation of bisphenol A (BPA). The catalytic test were performed by irradiating a polluted solution with a UV lamp having a maximum emission peak $\lambda = 312$ nm. The results that were obtained during the photodegradation tests evidenced that the PVDF/ TiO_2 PM hot-pressed at 100°C (PVDF/ TiO_2 -100), permitted to obtain a higher UV absorbance and pure water flux in comparison with the PMs PVDF/ TiO_2 -160 and PVDF/ TiO_2 -180 hot pressed at higher temperatures. This is because the morphological structure of the nanocomposite PMs was strongly influenced by the hot pressing temperature. In particular, the structure density of the PMs increased with the hot pressing temperature. Good BPA photodegradation (84.53%) was obtained by using the PVDF/ TiO_2 -100 under UV for 300 min, followed by PVDF/ TiO_2 -160 (77.61% BPA degradation) and PVDF/ TiO_2 -180 (62.54% BPA degradation). These results evidenced that the introduction of TiO_2 -NFs in on PVDF supports via hot pressing is a preparation method, which permits obtaining an enhanced photodegradation of organic pollutants, such as BPA.

Ramasundaram et al. [80] prepared TiO_2 -NFs integrated stainless steel filter (SSF) by some sequential steps (Figure 5), which also included a hot-pressing step. First of all, a free-standing TiO_2 -NFs layer was electrospun. The so prepared layer was then bounded to SSF surface by a hot pressing process while using PVDF nanofibers (PVDF-NFs) interlayer as a binder. Five different thicknesses of PVDF-NFs layer were considered in order to evaluate the influence of this parameter on the stability and the activity of the prepared SSF PMs. The stability of the five different SSF PMs was evaluated by submitting to sonication for 30 min five solutions containing them in water. The obtained results evidenced that 42 nm was the optimal PVDF-NFs layer for firmly bounding the TiO_2 -NFs to the surface of SSF.

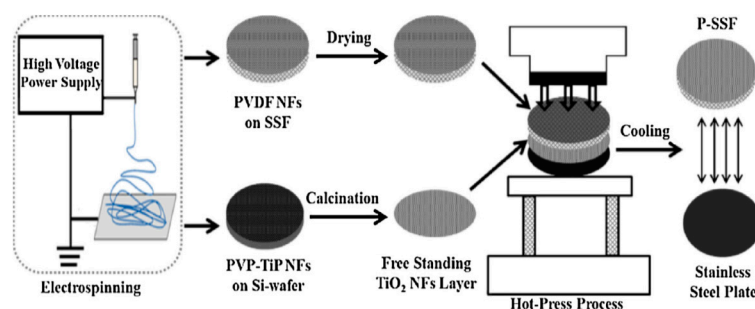


Figure 5. Schematization of the preparation process used for preparing the stainless steel filter PMs (SSF PMs) [80].

The photocatalytic performance of the so prepared and characterized PMs was tested in the degradation of cimetidine (CMD), a molecule of pharmaceutical interest, in an experimental set-up operated in dead-end mode. The results evidenced that the CMD photodegradation increased from 42% to 90% when the thickness of TiO₂-NFs increased from 10 to 29 mm. A further increase of the thickness did not have significant effect on drug degradation. This trend was probably due to the decreased light penetration. Moreover, CMD photodegradation was influenced by water flux across the membrane. In particular, it decreased from 89% to 64% and 47% by increasing the permeation flux from 10 to 20 and then 50 L·h⁻¹·m⁻². This trend can be explained by considering that, when the permeation flux increases, the contact time between the photocatalytic TiO₂ layer and drug molecules is decreased, resulting in the observed lower photodegradation.

Metal doping of TiO₂ photocatalyst, thanks to the passage of the promoted electron from the CB of the photocatalyst to that one of the metal, enhances: (i) the photocatalytic activity under visible light by reducing the band gap and (ii) the photocatalytic efficiency by minimizing the recombination of electron–hole couples. On these bases, Liu et al. [82] prepared an Ag/TiO₂-NF PM and tested it in the photocatalytic degradation of MB using a solar simulator (Xenon arc lamp) as the light source. These Ag/TiO₂-NF PMs permitted to obtain advanced performance in terms of both membrane fouling and loss of photocatalytic efficiency. Those enhancements were ascribed to the uniform dispersion of Ag NPs on TiO₂-NFs, while maintaining sufficient active sites. The latter achievement was evidenced by Brunauer-Emmet-Teller (BET) measurements (see Table 2): an increased BET specific surface area was obtained by doping with Ag the TiO₂-NFs (102.3 m²·g⁻¹ vs. 85.6 m²·g⁻¹). According to these data, the photocatalytic activity under solar irradiation of the Ag/TiO₂-NF membrane (expressed in terms of MB degradation rate constant (min⁻¹)) was significantly enhanced. As a consequence, 30 min of solar irradiation were enough to obtain a MB removal of nearly 80%. Complete mineralization was obtained after 80 min.

Table 2. MB degradation rate constant under solar irradiation by using different TiO₂-based photocatalytic membranes (Data from Liu et al. [82]).

	BET Specific Surface Area (m ² ·g ⁻¹)	MB Degradation Rate Constant (min ⁻¹)
Ag/TiO ₂ -nanofiber membrane	102.3	0.0211
TiO ₂ -nanofiber membrane	85.6	0.0137
P25 membrane	/	0.0076

The results that were obtained by Liu et al. [82] show that the intrinsic diminution of the photocatalytic activity of a PMR using immobilized instead of suspended photocatalyst, caused by presence of the polymeric chain around the particles of catalyst, can be minimized by using NF based PMs, thanks to their high surface area.

Concerning the other classical drawbacks of photocatalyst immobilization, i.e., photocatalyst leaching, Liu et al. [82] found an excellent reusability of the prepared PMs. Indeed, the photocatalytic

activity did not decrease during five successive photocatalytic runs. Moreover, the intrinsic antibacterial capability of the Ag/TiO₂-NF PMs could have a benefic effect with respect to control of the membrane biofouling, which is an important achievement in view of large scale applications.

A different approach to effectively disperse the photocatalyst particle into a PM was developed by Fischer et al. [83]. By hydrolysis of titanium tetraisopropoxide, TiO₂ NPs were formed directly onto the surface of two PES and PVDF hydrophilic membranes, and one PVDF hydrophobic membrane. By means of this method, a thin layer of disaggregated TiO₂ NPs was directly synthesized on membrane surface, thus achieving a strong binding between the photocatalyst and the membrane supports. The photocatalytic performance of the prepared PMs was studied by considering the photodegradation of three different pollutants, the dye MB and two drugs (ibuprofen (IBU) and diclofenac (DCF)). On the basis of the results it can be affirmed that the properties of pollutant adsorption gave a greater contribution with respect to TiO₂ content onto the PM. Indeed, better photocatalytic performances (70% MB photodegradation) were obtained with the hydrophilic TiO₂/PVDF PM, despite its lower TiO₂ content with respect to the TiO₂/PES PM (0.092% vs. 0.809%). The worst performance was obtained by using the hydrophobic PVDF-modified membrane. This trend was ascribed to the lower contact with MB, which was dissolved in water. Lower photodegradation efficiencies were obtained for DCF and IBU (68% and 44%, respectively), because of their higher concentration in water. An acceptable permeate quality was obtained after two or more permeate recycles. The stability of the photocatalytic performance of the prepared PMs was also tested. The results evidenced a complete stability of PMs after five successive runs obtaining the complete photocatalytic degradation of MB without damaging the PMs. This important achievement was due to the complete covering of the support by the TiO₂ layer, thus avoiding the direct irradiation of the polymeric support with UV irradiation.

Another possible way to overcome the intrinsic limitations of PMs is represented by the use of TiO₂ nanotubes (TiO₂ NTs). Fundamental characteristics in view of achieving excellent photocatalytic performance are their high surface area/volume ratio, short distance for charge carrier diffusion, and high photon-collection efficiency. Fischer et al. [84] prepared nanotubular TiO₂-PES membranes. The prepared PMs were tested for degrading DCF under UV light. The photocatalytic tests were carried by using two different operating modes: a static mode, i.e., with the membrane operating only as a photocatalytic support, and dead-end mode. A significant lower degradation rate constant was obtained by using the dead end mode with respect to the static mode (0.085×10^{-3} vs. $9.96 \times 10^{-3} \text{ min}^{-1}$). This difference was ascribed to consideration that, during the dead-end flow tests, only 20% of the solution was irradiated, while the remaining 80%, contained in the feed tank and tubes, was not irradiated. This consideration permit to introduce an important parameter to be appropriately considered in view of yielding satisfactory degradation rates: the ratio between the irradiated and the not irradiated volume.

4.2. Polyoxometalates-Based Photocatalytic Membranes

An interesting example of photocatalytic membrane preparation is the heterogenization in/on polymeric membranes of the polyoxometalate decatungstate (W₁₀O₃₂⁴⁻). POM are polyanionic metal oxide clusters of early transition metals [85], having promising properties for application in oxidation reactions for fine chemistry and wastewater treatments.

Decatungstate shows remarkable properties for the photocatalytic treatment of wastewater since its absorption spectrum, characterized by a maximum absorption at 324 nm, partially overlaps the solar emission spectrum opening the potential route for an environmentally friendly solar-assisted application [86]. The decatungstate-promoted photocatalysis is a multi-step process that can occur by substrate activation, or, when the reaction is carried out in water, by solvent activation (Figure 6) [86,87]. The dioxygen intercepts the organic radicals giving rise to an autooxidation chain, and provides the re-oxidation of the photocatalyst closing the cycle.

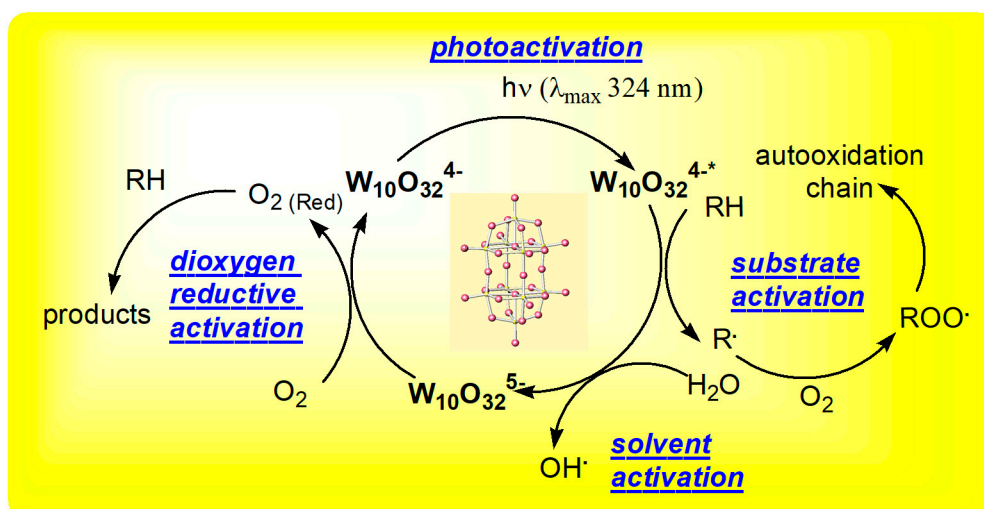


Figure 6. Schematization of the decatungstate-promoted photocatalysis in water [87].

However, decatungstate has also some relevant limitations, like: low quantum yields, small surface area, poor selectivity, and limited stability at pH higher than 2.5 [88,89]. Membrane technology can contribute to overcome these limitations by: the multi-turnover recycling of the heterogeneous photocatalyst, the possibility to tune reaction selectivity as a function of the substrate-membrane affinity, moreover, the structured polymeric micro-environment that is offered by the membrane can influence catalyst stability and activity.

In this perspective, innovative heterogeneous photo-oxygenation systems able to employ visible light, oxygen, mild temperatures, and solvent with a low environmental impact (like water or neat reactions), were designed and developed by the immobilization of decatungstate and other POMs in polymeric membranes made of polydimethylsiloxane (PDMS), PVDF, and Hyflon (Figure 7) [87,90–93].

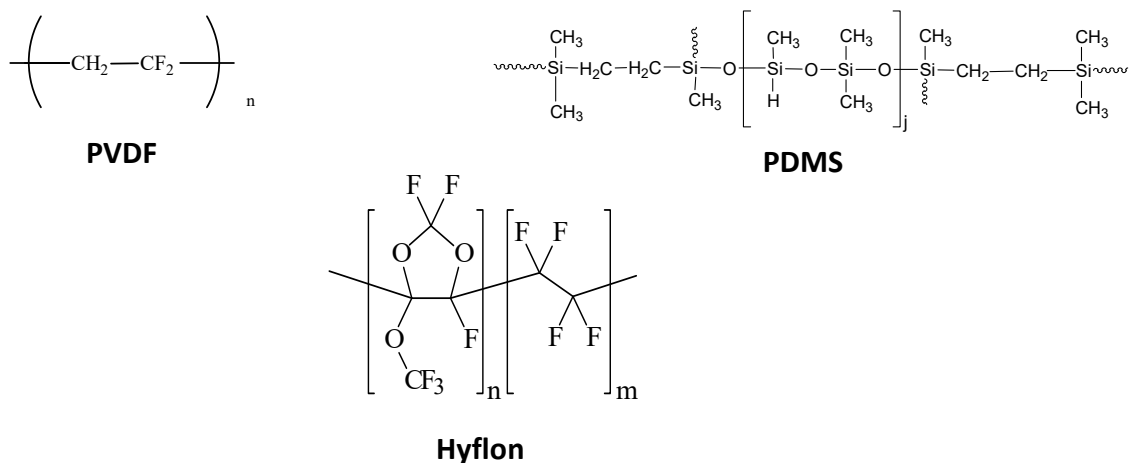


Figure 7. Chemical formula of the polymers used as membrane materials for the heterogenization of polyoxometalates.

These polymers were selected because they are transparent in the region of interest of the catalyst and are characterized by a high chemical, thermal and photostability. Moreover, in the case of PVDF and Hyflon, the use of a fluorinated media to carry out aerobic oxidation reactions is particularly useful because the high solubility of oxygen in fluorinated environment.

With the aim to improve the catalyst/polymer interactions, and to avoid catalyst leaching out from the membrane, lipophilic (insoluble in water) derivatives of the decatungstate were employed:

the tetrabutylammonium salt $((n\text{-C}_4\text{H}_9\text{N})_4\text{W}_{10}\text{O}_{32})$ indicated as TBAW10) and a fluorine-tagged decatungstate, $([\text{CF}_3(\text{CF}_2)_7(\text{CH}_2)_3]_3\text{CH}_3\text{N})_4\text{W}_{10}\text{O}_{32}$, indicated as $(\text{R}_f\text{N})_4\text{W}_{10}\text{O}_{32}$.

The photocatalytic membranes prepared were characterized by different and tailored properties depending on the nature and structure of the polymeric micro-environment in which the catalyst was immobilized.

Solid state characterization techniques, like FT-IR and UV-vis spectroscopy, confirmed that the structure and spectroscopic properties of the catalyst were preserved in the heterogenized form. The results evidenced as the appropriate catalyst/polymer design allowed for realizing new heterogeneous photocatalysts for the oxidation of organic substrates performed under oxygen atmosphere at room temperature, with improved performance concerning catalyst's stability and selectivity than the analogous homogeneous reactions.

A membrane induced discrimination of the substrate was observed in the oxidations of a series of alcohols at different molecular weight and polarity carried with PDMS- and PVDF-based catalytic membranes containing TBAW10 operating in a batch setup while using a Hg-Xe arc lamp as light source [87]. The alcohol oxidation occurred following a degradation pathway in which the aldehyde was formed as an intermediate [87].

PVDF membranes containing TBAW10 were also successfully used in the aerobic mineralization of phenol in water carried out in a continuous flow-through photocatalytic membrane reactors [92] operating with a mercury vapor lamp, emitting from 310 nm to visible light. The results indicate that the photocatalytic membrane were stable and recyclable in successive runs [92].

The catalyst heterogenization was carried out by solubilizing the catalyst into the polymer dope solution using a common solvent (dimethylacetamide) to prepare nano-hybrid membrane (PVDF-W10) by the phase separation technique. The catalytic membranes were characterized by a homogeneous distribution of the catalyst in membrane, as evident from SEM in back scattered electrons mode (BSE) and linear RX maps on the cross sections.

The catalyst stability was positively influenced by the polymeric environment, in which it was confined. Moreover, the selective separation function of the membrane resulted in an enhancement of the phenol mineralization in comparison with an analogous homogeneous reaction carried out with sodium salt of the decatungstate [92]. The dependence of the phenol degradation rate by the catalyst loading in membrane and the transmembrane pressure was investigated, allowing to identify the catalytic membrane with catalyst loading 25.0 wt.% and operating at 1 bar (contact time 22 s), as the more efficient system [92].

The rates of phenol degradation catalysed by homogenous $\text{Na}_4\text{W}_{10}\text{O}_{32}$ and heterogeneous PVDF-W10 (25.0 wt.%) were compared in similar operative conditions. The percentages of phenol degraded in the homogeneous and heterogeneous reaction were similar. In both cases, after 5 h, about 50% of the phenol was converted. However, in the case of the homogenous reaction various persistent intermediates (e.g., benzoquinone, hydroquinone, and catechol) were observed and only the 34.0% of mineralization to CO_2 and water was achieved. On the contrary, during photodegradation performed by PVDF catalytic membrane, the phenol converted was completely mineralized to CO_2 and H_2O .

The higher catalytic activity of the PVDF-W10 membranes, in comparison to the homogeneous catalyst, was ascribed to the selective absorption of the organic substrate from water on the hydrophobic PVDF polymer membrane that increased the effective phenol concentration around the catalytic sites, optimizing the catalyst-substrate contact in the flow-through PMR.

Moreover, the polymeric hydrophobic environment protected the decatungstate from the conversion to an isomer, which absorbs only light under 280 nm, which instead occurs in homogeneous solution at $\text{pH} > 2.5$ [89,92].

Polymeric catalytic membranes were also prepared by immobilizing sodium decatungstate ($\text{Na}_4\text{W}_{10}\text{O}_{32}$; W10) [94,95] and phosphotungstic acid ($\text{H}_3\text{PW}_{12}\text{O}_{40}$; W12) [91], on the surface of PVDF membranes functionalized by Ar/ NH_3 plasma discharges (PVDF- NH_2).

Polar chemical groups (mainly NH_2 , but also OH, CN, NH, and CO) were grafted by a NH_3 plasma discharge on the upper surface of PVDF membranes [91,94,95], pre-treated with Ar in order to control hydrophobic recovery phenomena [96].

The groups grafted on the membrane surface were able to interact with the POMs solubilized in the aqueous solution, forming charge transfer complexes.

Surface-diagnostic techniques, such as X-ray photoelectron spectroscopy, contact angle measurements (CA), and RX maps, were used to support the successfully surface modification.

The catalytic membranes obtained showed superior performances (higher reaction rates) when compared to the corresponding homogeneous catalysts, in the aerobic phenol degradation reaction [91,94,95].

Decatungstate was also heterogenized in membrane made of Hyflon, an amorphous perfluoro co-polymer. It is important to note that the TBAW10 formed irregular catalyst aggregates in Hyflon membranes because of the low affinity with the polymeric matrix. However, the affinity between the polymer and the catalyst was improved by an appropriate functionalization of the second one. The fluorine-tagged $(\text{R}_f\text{N})_4 \text{W}_{10}\text{O}_{32}$, was well dispersed in the Hyflon membranes as spherical clusters with uniform size.

The cationic amphiphilic R_fN^+ groups induced the self-assembly of the surfactant-encapsulated clusters (i.e., R_fN^+ groups capped on $\text{W}_{10}\text{O}_{32}^{4-}$) which, during membrane formation process, gave supramolecular assemblies of the catalyst, stabilized by the polymeric matrix.

This self-assembling process was tuned by a proper choice of the membrane preparation conditions, like polymer concentration, catalyst loading, cast film thickness, and temperature [9].

The Hyflon-based catalytic membranes were applied in the solvent-free photo-oxygenation of benzylic C-H bonds with up to 6100 turnover number (moles of products for moles of catalyst) in 4 h and remarkable alcohol selectivity, thus providing a convenient alternative to other radical centered oxygenation systems [94].

5. Conclusions

In the last years, significant progresses were reached in the design and development photocatalytic membranes and photocatalytic membrane reactors.

PMRs are reactive separations that realize functional synergies between a membrane-based separation process and a photocatalytic conversion in agreement with the fundamentals of the process intensification strategy. However, significant improvements in membranes performance and durability, as well as plant design optimization, are still required in order to reach a mature technological stage and offer a real challenge to conventional photocatalytic systems in the perspective of the realization of a sustainable growth.

TiO_2 is the most widely investigated photocatalyst in PMRs. This photocatalyst is used in two main configurations: (i) dispersed in solution and compartmentalized in the reactors by the membrane; and, (ii) immobilized in or on the photocatalytic membrane.

However, interesting results were also achieved with photocatalytic membranes functionalized with polyoxometalates applied into oxidation reactions for wastewater treatment and fine chemistry.

The design and realization of photocatalytic membranes by the immobilization of a photocatalyst in/on a membrane, is characterized by relevant technical complexities but these systems can lead specific advantages in terms of productivity and sustainability in comparison to traditional heterogeneous photocatalysts.

Main issues to be addressed are the development of tailored photocatalytic membranes and membrane modules with acceptable costs, stable in a wide range of operative conditions, resistant to fouling, and showing high and reproducible performance over long terms.

Author Contributions: E.F. and P.A. elaborated the literature overview, wrote and revised the paper; E.D. and R.M. participated in valuable discussion and gave insightful comments on the work.

Funding: This research received no external funding.

Conflicts of Interest: The authors declare no conflict of interest.

Abbreviation

AOPs	advanced oxidation processes
BAT	best available technology
BCFM	binary composite fiber membrane
BPA	bisphenol A
BET	Brunauer-Emmet-Teller
CHD	chlorhexidine digluconate
CMD	cimetidine
CB	conduction band
DCF	diclofenac
DB	direct black 168
DW	distilled water
DMF	<i>N,N</i> -dimethylformamide
GO-TiO ₂	graphene oxide doped TiO ₂
HF	hollow fiber
IBU	ibuprofen
MBR	membrane bioreactor
MR	membrane reactor
MB	methylene blue
MO	methyl orange
MWCO	molecular weight cut off
MWCNT	multi-walled carbon nanotubes
NP	nanoparticle
NT	nanotube
N-TiO ₂	nitrogen doped TiO ₂
PM	photocatalytic membrane
PMR	photocatalytic membrane reactor
PAN	polyacrylonitrile
PDMS	polydimethylsiloxane
PES	polyethersulfone
PET	polyethylene terephthalate
POMs	polyoxometalates
PTFE	polytetrafluoroethylene
PU	polyurethane
PVC	polyvinylchloride
PVDF	polyvinylidene fluoride
P(VDF-TrFE)	poly(vinylidene fluoride–trifluoroethylene)
PI	process intensification
(R _f N) ₄ W ₁₀ O ₃₂	[CF ₃ (CF ₂) ₇ (CH ₂) ₃] ₃ CH ₃ N) ₄ W ₁₀ O ₃₂
RhB	rhodamine B
SEM	scanning electron microscopy
SBW	simulated brackish water
SSF	stainless steel filter
TBAW10	(n-C ₄ H ₉ N) ₄ W ₁₀ O ₃₂
TCFMs	ternary composite fiber membranes
TiO ₂ NTs	TiO ₂ nanotubes

TNF	titanium dioxide nanofiber
TOC	total organic carbon
UF	ultrafiltration
UF-PM	photocatalytic UF membrane
UV	ultraviolet
VB	valence band
XRD	X-ray diffraction
WSC	water-soluble chitosan

References

- Sanchez Marcano, J.G.; Tsotsis, T.T. Membrane Reactors. In *Ullmann's Encyclopedia of Industrial Chemistry*; Wiley-VCH: Weinheim, Germany, 2005; ISBN 9783527303854.
- Wöltinger, J.; Karau, A.; Leuchtenberger, W.; Drauz, K. Membrane Reactors at Degussa. In *Technology Transfer in Biotechnology. Advances in Biochemical Engineering*; Kragl, U., Ed.; Springer: Berlin, Germany, 2005; Volume 92, ISBN 978-3-540-22412-9. [[CrossRef](#)]
- Ibrahim, M.H.; El-Naas, M.H.; Zhang, Z.; Van der Bruggen, B. CO₂ Capture Using Hollow Fiber Membranes: A Review of Membrane Wetting. *Energy Fuels* **2018**, *32*, 963–978. [[CrossRef](#)]
- Le-Clech, P.; Chen, V.; Fane, T.A.G. Fouling in membrane bioreactors used in wastewater treatment. *J. Membr. Sci.* **2006**, *284*, 17–53. [[CrossRef](#)]
- Charpentier, J.-C. Modern Chemical Engineering in the Framework of Globalization, Sustainability, and Technical Innovation. *Ind. Eng. Chem. Res.* **2007**, *46*, 3465–3485. [[CrossRef](#)]
- Stankiewicz, A. Reactive separations for process intensification: An industrial perspective. *Chem. Eng. Process.* **2003**, *42*, 137–144. [[CrossRef](#)]
- Drioli, E.; Stankiewicz, A.; Macedonio, F. Membrane engineering in process intensification—An overview. *J. Membr. Sci.* **2011**, *380*, 1–8. [[CrossRef](#)]
- Sirkar, K.K.; Shanbhag, P.V.; Kovvali, A.S. Membrane in a Reactor: A Functional Perspective. *Ind. Eng. Chem. Res.* **1999**, *38*, 3715–3737. [[CrossRef](#)]
- Fontananova, E.; Drioli, E. Catalytic Membranes and Membrane Reactors. In *Comprehensive Membrane Science and Engineering*; Drioli, E., Giorno, L., Eds.; Elsevier: Oxford, UK, 2010; Volume 3, pp. 109–133, ISBN 978-0-08-093250-7.
- Vankelecom, I.F.J. Polymeric Membranes in Catalytic Reactors. *Chem. Rev.* **2002**, *102*, 3779–3810. [[CrossRef](#)] [[PubMed](#)]
- Molinari, R.; Marino, T.; Argurio, P. Photocatalytic membrane reactors for hydrogen production from water. *Int. J. Hydrogen Energy* **2014**, *39*, 7247–7261. [[CrossRef](#)]
- Zheng, X.; Shen, Z.-P.; Shi, L.; Cheng, R.; Yuan, D.-Y. Photocatalytic Membrane Reactors (PMRs) in Water Treatment: Configurations and Influencing Factors. *Catalysts* **2017**, *7*, 224. [[CrossRef](#)]
- Mozia, S. Photocatalytic membrane reactors (PMRs) in water and wastewater treatment. A review. *Sep. Purif. Technol.* **2010**, *73*, 71–91. [[CrossRef](#)]
- Molinari, R.; Lavorato, C.; Argurio, P. Recent progress of photocatalytic membrane reactors in water treatment and in synthesis of organic compounds. A review. *Catal. Today* **2017**, *281*, 144–164. [[CrossRef](#)]
- Dioos, B.M.L.; Vankelecom, I.F.J.; Jacobs, P.A. Aspects of Immobilisation of Catalysts on Polymeric Supports. *Adv. Synth. Catal.* **2006**, *348*, 1413–1446. [[CrossRef](#)]
- Molinari, R.; Lavorato, C.; Argurio, P. Photocatalytic reduction of acetophenone in membrane reactors under UV and visible light using TiO₂ and Pd/TiO₂ catalysts. *Chem. Eng. J.* **2015**, *274*, 307–316. [[CrossRef](#)]
- Sclafani, A.; Palmisano, L.; Schiavello, M. Phenol and nitrophenol photodegradation using aqueous TiO₂ dispersions. In *Aquatic and Surface Photochemistry*; Helz, G.R., Zepp, R.G., Crosby, D.G., Eds.; Lewis Publishers: London, UK, 1994; p. 419. [[CrossRef](#)]
- Hairom, N.H.H.; Mohammad, A.W.; Kadhum, A.A.H. Effect of various zinc oxide nanoparticles in membrane photocatalytic reactor for Congo red dye treatment. *Sep. Purif. Technol.* **2014**, *137*, 74–81. [[CrossRef](#)]
- Molinari, R.; Caruso, A.; Argurio, P.; Poerio, T. Degradation of the drugs Gemfibrozil and Tamoxifen in pressurized and de-pressurized membrane photoreactors using suspended polycrystalline TiO₂ as catalyst. *J. Membr. Sci.* **2008**, *319*, 54–63. [[CrossRef](#)]

20. Lavorato, C.; Argurio, P.; Mastropietro, T.F.; Pirri, G.; Poerio, T.; Molinari, R. Pd/TiO₂ doped faujasite photocatalysts for acetophenone transfer hydrogenation in a photocatalytic membrane reactor. *J. Catal.* **2017**, *353*, 152–161. [[CrossRef](#)]
21. Brunetti, A.; Barbieri, G.; Drioli, E. Upgrading of a syngas mixture for pure hydrogen production in a Pd–Ag membrane reactor. *Chem. Eng. Sci.* **2009**, *64*, 3448–3454. [[CrossRef](#)]
22. Song, H.; Shao, J.; He, Y.; Liu, B.; Zhong, X. Natural organic matter removal and flux decline with PEG–TiO₂-doped PVDF membranes by integration of ultrafiltration with photocatalysis. *J. Membr. Sci.* **2012**, *405–406*, 48–56. [[CrossRef](#)]
23. Wang, W.Y.; Irawan, A.; Ku, Y. Photocatalytic degradation of Acid Red 4 using a titanium dioxide membrane supported on a porous ceramic tube. *Water Res.* **2008**, *42*, 4725–4732. [[CrossRef](#)] [[PubMed](#)]
24. Iglesias, O.; Rivero, M.J.; Urriaga, A.M.; Ortiz, I. Membrane-based photocatalytic systems for process intensification. *Chem. Eng. J.* **2016**, *305*, 136–148. [[CrossRef](#)]
25. Horovitz, I.; Avisar, D.; Baker, M.A.; Grilli, R.; Lozzi, L.; Di Camillo, D.; Mamane, H. Carbamazepine degradation using a N-doped TiO₂ coated photocatalytic membrane reactor: Influence of physical parameters. *J. Hazard. Mater.* **2016**, *310*, 98–107. [[CrossRef](#)] [[PubMed](#)]
26. Athanasekou, C.P.; Moustakas, N.G.; Morales-Torres, S.; Pastrana-Martínez, L.M.; Figueiredo, J.L.; Faria, J.L.; Silva, A.M.T.; Dona-Rodríguez, J.M.; Romanos, G.E.; Falaras, P. Ceramic Photocatalytic Membranes for Water Filtration Under UV and Visible Light. *Appl. Catal. B Environ.* **2015**, *178*, 12–19. [[CrossRef](#)]
27. Pastrana-Martínez, L.M.; Morales-Torres, S.; Figueiredo, J.L.; Faria, J.L.; Silva, A.M.T. Graphene Oxide Based Ultrafiltration Membranes for Photocatalytic Degradation of Organic Pollutants in Salty Water. *Water Res.* **2015**, *77*, 179–190. [[CrossRef](#)] [[PubMed](#)]
28. Misra, A.J.; Das, S.; Habeeb Rahman, A.P.; Das, B.; Jayabalan, R.; Behera, S.K.; Suar, M.; Tamhankar, A.J.; Mishra, A.; Lundborg, C.S.; et al. Doped ZnO nanoparticles impregnated on Kaolinite (Clay): A reusable nanocomposite for photocatalytic disinfection of multidrug resistant *Enterobacter* sp. under visible light. *J. Colloid Interface Sci.* **2018**, *530*, 610–623. [[CrossRef](#)] [[PubMed](#)]
29. Najma, B.; Kasi, A.K.; Khan Kasi, J.; Akbar, A.; Bokhari, S.M.A.; Stroe, I.R. ZnO/AAO photocatalytic membranes for efficient water disinfection: Synthesis, characterization and antibacterial assay. *Appl. Surf. Sci.* **2018**, *448*, 104–114. [[CrossRef](#)]
30. Peyravi, M.; Jahanshahi, M.; Khalili, S. Fouling of WO₃ nanoparticle-incorporated PSf membranes in ultrafiltration of landfill leachate and dairy a combined wastewaters: An investigation using model. *Chin. J. Chem. Eng.* **2017**, *25*, 741–751. [[CrossRef](#)]
31. Alzahrani, E. Chitosan membrane embedded with ZnO/CuO nanocomposites for the photodegradation of fast green dye under artificial and solar irradiation. *Anal. Chem. Insights* **2018**, *13*. [[CrossRef](#)] [[PubMed](#)]
32. Katsoulis, D.E. A Survey of Applications of Polyoxometalates. *Chem. Rev.* **1998**, *98*, 359–388. [[CrossRef](#)] [[PubMed](#)]
33. Herrmann, J.-M. Heterogeneous Photocatalysis: State of the Art and Present Applications. *Top. Catal.* **2005**, *34*, 49–65. [[CrossRef](#)]
34. Brosillon, S.; Lhomme, L.; Vallet, C.; Bouzaza, A.; Wolbert, D. Gas Phase Photocatalysis and Liquid Phase Photocatalysis: Interdependence and Influence of Substrate Concentration and Photon Flow on Degradation Reaction Kinetics. *Appl. Catal. B Environ.* **2008**, *78*, 232–241. [[CrossRef](#)]
35. Sabaghi, V.; Davar, F.; Fereshteh, Z. ZnS nanoparticles prepared via simple reflux and hydrothermal method: Optical and photocatalytic properties. *Ceram. Int.* **2018**, *44*, 7545–7556. [[CrossRef](#)]
36. Zhang, W.; Ding, L.; Luo, J.; Jaffrin, M.Y.; Tang, B. Membrane fouling in photocatalytic membrane reactors (PMRs) for water and wastewater treatment: A critical review. *Chem. Eng. J.* **2016**, *302*, 446–458. [[CrossRef](#)]
37. Reddy, N.L.; Rao, V.N.; Kumari, M.M.; Kakarla, R.R.; Ravi, P.; Sathish, M.; Karthik, M.; Venkatakrishnan, S.M.; Inamuddin. Nanostructured semiconducting materials for efficient hydrogen generation. *Environ. Chem. Lett.* **2018**, *16*, 765–796. [[CrossRef](#)]
38. Yamani, Z.H. Comparative Study on Photocatalytic Degradation of Methylene Blue by Degussa P25 Titania: Pulsed Laser Light Versus Continuous Broad Spectrum Lamp Irradiation. *Arab. J. Sci. Eng.* **2018**, *43*, 423–432. [[CrossRef](#)]
39. Hayat, K.; Gondal, M.A.; Khaleda, M.M.; Yamani, Z.H.; Ahmed, S. Laser induced photocatalytic degradation of hazardous dye (Safranin-O) using self synthesized nanocrystalline WO₃. *J. Hazard. Mater.* **2011**, *186*, 1226–1233. [[CrossRef](#)] [[PubMed](#)]

40. Li, S.; Lin, Q.; Liu, X.; Yang, L.; Ding, J.; Dong, F.; Li, Y.; Irfana, M.; Zhang, P. Fast photocatalytic degradation of dyes using low power laser-fabricated Cu₂O–Cu nanocomposites. *RSC Adv.* **2018**, *8*, 20277–20286. [[CrossRef](#)]
41. Dominguez, S.; Laso, J.; Margallo, M.; Aldaco, R.; Rivero, M.J.; Irabien, Á.; Ortiz, I. LCA of greywater management within a water circular economy restorative thinking framework. *Sci. Total Environ.* **2018**, *621*, 1047–1056. [[CrossRef](#)] [[PubMed](#)]
42. Aoudjit, L.; Martins, P.M.; Madjene, F.; Petrovykh, D.Y.; Lanceros-Mendez, S. Photocatalytic reusable membranes for the effective degradation of tartrazine with a solar photoreactor. *J. Hazard. Mat.* **2018**, *344*, 408–416. [[CrossRef](#)] [[PubMed](#)]
43. Halim, R.; Utama, R.; Cox, S.; Le-Clech, P. Performances of submerged membrane photocatalysis reactor during treatment of humic substances. *Membr. Water Treat.* **2010**, *1*, 283–296. [[CrossRef](#)]
44. Song, L.; Zhu, B.; Jegatheesan, V.; Gray, S.; Duke, M.; Muthukumar, S. Treatment of secondary effluent by sequential combination of photocatalytic oxidation with ceramic membrane filtration. *Environ. Sci. Pollut. Res.* **2018**, *25*, 5191–5202. [[CrossRef](#)] [[PubMed](#)]
45. Tang, T.; Lu, G.; Wang, W.; Wang, R.; Huang, K.; Qiu, Z.; Tao, X.; Dang, Z. Photocatalytic removal of organic phosphate esters by TiO₂: Effect of inorganic ions and humic acid. *Chemosphere* **2018**, *206*, 26–32. [[CrossRef](#)] [[PubMed](#)]
46. Borthakur, P.; Das, M.R. Hydrothermal assisted decoration of NiS₂ and CoS nanoparticles on the reduced graphene oxide nanosheets for sunlight driven photocatalytic degradation of azo dye: Effect of background electrolyte and surface charge. *J. Colloid Interface Sci.* **2018**, *516*, 342–354. [[CrossRef](#)] [[PubMed](#)]
47. Augugliaro, V.; Litter, M.; Palmisano, L.; Soria, J. The Combination of Heterogeneous Photocatalysis With Chemical and Physical Operations: A Tool for Improving the Photoprocess Performance. *J. Photochem. Photobiol. C Photochem. Rev.* **2006**, *7*, 127–144. [[CrossRef](#)]
48. Darowna, D.; Wróbel, R.; Morawski, A.W.; Mozia, S. The influence of feed composition on fouling and stability of a polyethersulfone ultrafiltration membrane in a photocatalytic membrane reactor. *Chem. Eng. J.* **2017**, *310*, 360–367. [[CrossRef](#)]
49. Gladysz, J.A. Recoverable catalysts. Ultimate goals, criteria of evaluation, and the green chemistry interface. *Pure Appl. Chem.* **2001**, *73*, 1319–1324. [[CrossRef](#)]
50. Hill, C.L. Homogeneous catalysis. Controlled green oxidation. *Nature* **1999**, *401*, 436–437. [[CrossRef](#)] [[PubMed](#)]
51. Daels, N.; Radoicic, M.; Radetic, M.; Van Hulle, S.W.; De Clerck, K. Functionalisation of electrospun polymer nanofibre membranes with TiO₂ nanoparticles in view of dissolved organic matter photodegradation. *Sep. Purif. Technol.* **2014**, *133*, 282–290. [[CrossRef](#)]
52. Wu, G.; Cui, L.; Xu, Y.; Lu, X. Photocatalytic membrane reactor for degradation of phenol in aqueous solution. *Fresenius Environ. Bull.* **2007**, *16*, 812–816.
53. Fischer, K.; Gawel, A.; Rosen, D.; Krause, M.; Latif, A.A.; Griebel, J.; Prager, A.; Schulze, A. Low-temperature synthesis of anatase/rutile/brookite TiO₂ nanoparticles on a polymer membrane for photocatalysis. *Catalysts* **2017**, *7*, 209. [[CrossRef](#)]
54. Kim, J.H.; Joshi, M.K.; Lee, J.; Park, C.H.; Kim, C.S. Polydopamine-assisted immobilization of hierarchical zinc oxide nanostructures on electrospun nanofibrous membrane for photocatalysis and antimicrobial activity. *J. Colloid Interface Sci.* **2018**, *513*, 566–574. [[CrossRef](#)] [[PubMed](#)]
55. Artoshina, O.V.; Rossouw, A.; Semina, V.K.; Nechaev, A.N.; Apel, P.Y. Structural and physicochemical properties of titanium dioxide thin films obtained by reactive magnetron sputtering, on the surface of track-etched membranes. *Pet. Chem.* **2015**, *55*, 759–768. [[CrossRef](#)]
56. Shi, Y.; Yang, D.; Li, Y.; Qu, J.; Yu, Z.-Z. Fabrication of PAN@TiO₂/Ag nanofibrous membrane with high visible light response and satisfactory recyclability for dye photocatalytic degradation. *Appl. Surf. Sci.* **2017**, *426*, 622–629. [[CrossRef](#)]
57. Li, N.; Tian, Y.; Zhang, J.; Sun, Z.; Zhao, J.; Zhang, J.; Zuo, W. Precisely-controlled modification of PVDF membranes with 3D TiO₂/ZnO nanolayer: Enhanced anti-fouling performance by changing hydrophilicity and photocatalysis under visible light irradiation. *J. Membr. Sci.* **2017**, *528*, 359–368. [[CrossRef](#)]
58. Mozia, S.; Darowna, D.; Wróbel, R.; Morawski, A.W. A study on the stability of polyethersulfone ultrafiltration membranes in a photocatalytic membrane reactor. *J. Membr. Sci.* **2015**, *495*, 176–186. [[CrossRef](#)]

59. Drioli, E.; Fontananova, E. Catalytic membranes embedding selective catalysts: Preparation and applications. In *Heterogenized Homogeneous Catalysts for Fine Chemicals Production: Materials and Processes*; Barbaro, P., Liguori, F., Eds.; Springer: Berlin, Germany, 2010; Chapter 6; ISBN 978-90-481-3696-4.
60. Strathmann, H.; Giorno, L.; Drioli, E. *An Introduction to Membrane Science and Technology*; CNR: Rome, Italy, 2006; ISBN 88-8080-063-9.
61. Wang, X.; Shi, F.; Huang, W.; Fan, C. Synthesis of high quality TiO₂ membranes on alumina supports and their photocatalytic activity. *Thin Solid Films* **2012**, *520*, 2488–2492. [[CrossRef](#)]
62. Chakraborty, S.; Loutatidou, S.; Palmisano, G.; Kujawa, J.; Mavukkandy, M.A.; Al-Gharabli, S.; Curcio, E.; Arafat, H.A. Photocatalytic hollow fiber membranes for the degradation of pharmaceutical compounds in wastewater. *J. Environ. Chem. Eng.* **2017**, *5*, 5014–5024. [[CrossRef](#)]
63. Nor, N.A.M.; Jaafar, J.; Ismail, A.F.; Mohamed, M.A.; Rahman, M.A.; Othman, M.H.D.; Lau, W.J.; Yusof, N. Preparation and performance of PVDF-based nanocomposite membrane consisting of TiO₂ nanofibers for organic pollutant decomposition in wastewater under UV irradiation. *Desalination* **2016**, *391*, 89–97. [[CrossRef](#)]
64. Kaijun, Z.; Qingshan, L.; Yu, W. Preparation and performance of PMMA/R-TiO₂ and PMMA/A-TiO₂ electrospun fibrous films. *Integr. Ferroelectr.* **2018**, *188*, 31–43. [[CrossRef](#)]
65. Fischer, K.; Gläser, R.; Schulze, A. Nanoneedle and nanotubular titanium dioxide–PES mixed matrix membrane for photocatalysis. *Appl. Catal. B Environ.* **2014**, *160*, 456–464. [[CrossRef](#)]
66. Della Foglia, F.; Chiarello, G.L.; Dozzi, M.V.; Piseri, P.; Bettini, L.G.; Vinati, S.; Ducati, C.; Milani, P.; Selli, E. Hydrogen production by photocatalytic membranes fabricated by supersonic cluster beam deposition on glass fiber filters. *Int. J. Hydrogen Energy* **2014**, *39*, 13098–13104. [[CrossRef](#)]
67. Zhang, E.; Wang, L.; Zhang, B.; Xie, Y.; Sun, C.; Jiang, C.; Zhang, Y.; Wang, G. Modification of polyvinylidene fluoride membrane with different shaped α -Fe₂O₃ nanocrystals for enhanced photocatalytic oxidation performance. *Mater. Chem. Phys.* **2018**, *214*, 41–47. [[CrossRef](#)]
68. Chen, Q.; Yu, Z.; Pan, Y.; Zeng, G.; Shi, H.; Yang, X.; Li, F.; Yang, S.; He, Y. Enhancing the photocatalytic and antibacterial property of polyvinylidene fluoride membrane by blending Ag–TiO₂ nanocomposites. *J. Mater. Sci.-Mater. Electron.* **2017**, *28*, 3865–3874. [[CrossRef](#)]
69. Hoseini, S.N.; Pirzaman, A.K.; Aroon, M.A.; Pirbazari, A.E. Photocatalytic degradation of 2,4-dichlorophenol by Co-doped TiO₂(Co/TiO₂) nanoparticles and Co/TiO₂ containing mixed matrix membranes. *J. Water Proc. Eng.* **2017**, *17*, 124–134. [[CrossRef](#)]
70. Rajeswari, A.; Vismaiya, S.; Pius, A. Preparation, characterization of nano ZnO-blended cellulose acetate-polyurethane membrane for photocatalytic degradation of dyes from water. *Chem. Eng. J.* **2017**, *313*, 928–937. [[CrossRef](#)]
71. Yin, J.; Deng, B. Polymer-matrix nanocomposite membranes for water treatment. *J. Membr. Sci.* **2015**, *479*, 256–275. [[CrossRef](#)]
72. Zhao, Y.; Ma, L.; Chang, W.; Huang, Z.; Feng, X.; Qi, X.; Li, Z. Efficient photocatalytic degradation of gaseous N,N-dimethylformamide in tannery waste gas using doubly open-ended Ag/TiO₂ nanotube array membranes. *Appl. Surf. Sci.* **2018**, *444*, 610–620. [[CrossRef](#)]
73. Papageorgiou, S.K.; Katsaros, F.K.; Favvas, E.P.; Romanos, G.E.; Athanasekou, C.P.; Beltsios, K.G.; Tziaila, O.I.; Falaras, P. Alginate Fibers as Photocatalyst Immobilizing Agents Applied in Hybrid Photocatalytic/Ultrafiltration Water Treatment Processes. *Water Res.* **2012**, *46*, 1858–1872. [[CrossRef](#)] [[PubMed](#)]
74. Anderson, M.A.; Gieselmann, M.J.; Xu, Q.J. Titania and Alumina Ceramic Membranes. *J. Membr. Sci.* **1988**, *39*, 243–258. [[CrossRef](#)]
75. Moosemiller, M.D.; Hill, C.G., Jr.; Anderson, M.A. Physicochemical Properties of Supported γ -Al₂O₃ and TiO₂ Ceramic Membranes. *Sep. Sci. Technol.* **1989**, *24*, 641–657. [[CrossRef](#)]
76. Molinari, R.; Palmisano, L.; Drioli, E.; Schiavello, M. Studies on Various Reactor Configurations for Coupling Photocatalysis and Membrane Processes in Water Purification. *J. Membr. Sci.* **2002**, *206*, 399–415. [[CrossRef](#)]
77. Zhang, H.; Quan, X.; Chen, S.; Zhao, H.; Zhao, Y. Fabrication of Photocatalytic Membrane and Evaluation Its Efficiency in Removal of Organic Pollutants From Water. *Sep. Purif. Technol.* **2006**, *50*, 147–155. [[CrossRef](#)]
78. Wang, Z.-B.; Guan, Y.-J.; Chen, B.; Bai, S.-L. Retention and Separation of 4BS Dye from Wastewater by the N-TiO₂ Ceramic Membrane. *Desalin. Water Treat.* **2016**, *57*, 16963–16969. [[CrossRef](#)]

79. Wu, X.-Q.; Shen, J.-S.; Zhao, F.; Shao, Z.-D.; Zhong, L.-B.; Zheng, Y.-M. Flexible electrospun MWCNTs/Ag₃PO₄/PAN ternary composite fiber membranes with enhanced photocatalytic activity and stability under visible-light irradiation. *J. Mater. Sci.* **2018**, *53*, 10147–10159. [[CrossRef](#)]
80. Ramasundaram, S.; Yoo, H.N.; Song, K.G.; Lee, J.; Choi, K.J.; Hong, S.W. Titanium Dioxide Nanofibers Integrated Stainless Steel Filter for Photocatalytic Degradation of Pharmaceutical Compounds. *J. Hazard. Mater.* **2013**, *258–259*, 124–132. [[CrossRef](#)] [[PubMed](#)]
81. Georgi, A.; Kopinke, F.-D. Interaction of Adsorption and Catalytic Reactions in Water Decontamination Processes: Part I. Oxidation of Organic Contaminants with Hydrogen Peroxide Catalyzed by Activated Carbon. *Appl. Catal. B Environ.* **2005**, *58*, 9–18. [[CrossRef](#)]
82. Liu, L.; Liu, Z.; Bai, H.; Sun, D.D. Concurrent Filtration and Solar Photocatalytic Disinfection/Degradation Using High-Performance Ag/TiO₂ Nanofiber Membrane. *Water Res.* **2012**, *46*, 1101–1112. [[CrossRef](#)] [[PubMed](#)]
83. Fischer, K.; Grimm, M.; Meyers, J.; Dietrich, C.; Gläser, R.; Schulze, A. Photoactive Microfiltration Membranes via Directed Synthesis of TiO₂ Nanoparticles on the Polymer Surface for Removal of Drugs From Water. *J. Membr. Sci.* **2015**, *478*, 49–57. [[CrossRef](#)]
84. Fischer, K.; Kuhnert, M.; Glaser, R.; Schulze, A. Photocatalytic Degradation and Toxicity Evaluation of Diclofenac by Nanotubular Titanium Dioxide–PES Membrane in a Static and Continuous Setup. *RSC Adv.* **2015**, *5*, 16340–16348. [[CrossRef](#)]
85. Pope, M. *Heteropoly and Isopoly Oxometalates*; Springer: New York, NY, USA, 1983; ISBN 978-3-662-12006-4.
86. Maldotti, A.; Molinari, A.; Amadelli, R. Photocatalysis with Organized Systems for the Oxofunctionalization of Hydrocarbons by O₂. *Chem. Rev.* **2002**, *102*, 3811–3836. [[CrossRef](#)] [[PubMed](#)]
87. Bonchio, M.; Carraro, M.; Scorrano, G.; Fontananova, E.; Drioli, E. Heterogeneous Photooxidation of Alcohols in Water by Photocatalytic Membranes Incorporating Decatungstate. *Adv. Synth. Catal.* **2003**, *345*, 1119–1126. [[CrossRef](#)]
88. Mylonas, A.; Papaconstantinou, E. Photocatalytic degradation of phenol and p-cresol by polyoxotungstates. Mechanistic implications. *Polyhedron* **1996**, *15*, 3211–3217. [[CrossRef](#)]
89. Texier, I.; Giannotti, C.; Malato, S.; Richter, C.; Delaire, J. Solar photodegradation of pesticides in water by sodium decatungstate. *Catal. Today* **1999**, *54*, 297–307. [[CrossRef](#)]
90. Bonchio, M.; Carraro, M.; Gardan, M.; Scorrano, G.; Drioli, E.; Fontananova, E. Hybrid photocatalytic membranes embedding decatungstate for heterogeneous photooxygenation. *Top. Catal.* **2006**, *40*, 133–140. [[CrossRef](#)]
91. Fontananova, E.; Donato, L.; Drioli, E.; Lopez, L.; Favia, P.; d’Agostino, R. Heterogenization of Polyoxometalates on the Surface of Plasma-Modified Polymeric Membranes. *Chem. Mater.* **2006**, *18*, 1561–1568. [[CrossRef](#)]
92. Drioli, E.; Fontananova, E.; Bonchio, M.; Carraro, M.; Gardan, M.; Scorrano, G. Catalytic Membranes and Membrane Reactors: An Integrated Approach to Catalytic Process with a High Efficiency and a Low Environmental Impact. *Chin. J. Catal.* **2008**, *29*, 1152–1158. [[CrossRef](#)]
93. Carraro, M.; Gardan, M.; Scorrano, G.; Drioli, E.; Fontananova, E.; Bonchio, M. Solvent-free, heterogeneous photooxygenation of hydrocarbons by Hyflon[®] membranes embedding a fluorine-tagged decatungstate: The importance of being fluorine. *Chem. Commun.* **2006**, *43*, 4533–4535. [[CrossRef](#)]
94. Lopez, L.C.; Buonomenna, M.G.; Fontananova, E.; Iacoviello, G.; Drioli, E.; d’Agostino, R.; Favia, P. A New Generation of Catalytic Poly(vinylidene fluoride) Membranes: Coupling Plasma Treatment with Chemical Immobilization of Tungsten-Based Catalysts. *Adv. Funct. Mater.* **2006**, *16*, 1417–1424. [[CrossRef](#)]
95. Lopez, L.C.; Buonomenna, M.G.; Fontananova, E.; Drioli, E.; Favia, P.; d’Agostino, R. Immobilization of Tungsten Catalysts on Plasma Modified Membranes. *Plasma Processes Polym.* **2007**, *4*, 326–333. [[CrossRef](#)]
96. Favia, P.; Sardella, E.; Gristina, R.; d’Agostino, R. Novel plasma processes for biomaterials: Micro-scale patterning of biomedical polymers. *Surf. Coat. Technol.* **2003**, *169–170*, 707–711. [[CrossRef](#)]

